EUROPEAN ORGANIZATION FOR NUCLEAR RESEARCH (CERN)

CERN-EP-2025-007
2025/12/04

CMS-HIG-23-011

Search for γH production and constraints on the Yukawa couplings of light quarks to the Higgs boson

The CMS Collaboration*

Abstract

A search for γH production is performed with data from the CMS experiment at the LHC corresponding to an integrated luminosity of 138 fb^{-1} at a proton-proton center-of-mass collision energy of 13 TeV. The analysis focuses on the topology of a boosted Higgs boson recoiling against a high-energy photon. The final states of $\text{H} \to \text{b}\bar{\text{b}}$ and $\text{H} \to 4\ell$ are analyzed. This study examines effective $\text{HZ}\gamma$ and $\text{H}\gamma\gamma$ anomalous couplings within the context of an effective field theory. In this approach, the production cross section is constrained to be $\sigma_{\gamma\text{H}} < 16.4$ fb at 95% confidence level (CL). Simultaneous constraints on four anomalous couplings involving $\text{HZ}\gamma$ and $\text{H}\gamma\gamma$ are provided. Additionally, the production rate for $\text{H} \to 4\ell$ is examined to assess potential enhancements in the Yukawa couplings between light quarks and the Higgs boson. Assuming the standard model values for the Yukawa couplings of the bottom and top quarks, the following simultaneous constraints are obtained: $\kappa_\text{u} = (0.0 \pm 1.5) \times 10^3$, $\kappa_\text{d} = (0.0^{+6.7}_{-6.8}) \times 10^2$, $\kappa_\text{s} = 0^{+30}_{-32}$, and $\kappa_\text{c} = 0.0^{+2.3}_{-2.8}$. This rules out the hypothesis that up- or down-type quarks in the first or second generation have the same Yukawa couplings as those in the third generation, with a CL greater than 95%.

Published in Physical Review D as doi:10.1103/6s8n-pvmy.

*See Appendix A for the list of collaboration members

1 Introduction

The observation of a Higgs boson (H) with a mass of 125 GeV by the ATLAS and CMS Collaborations [1–3] is consistent with the expectations from the standard model (SM) of particle physics [4–10]. Constraints on H boson spin-parity properties and anomalous couplings to electroweak gauge bosons $V = \gamma, Z, W$ (HVV couplings) have been set by the CMS [11–21] and ATLAS [22–30] experiments. The quantum numbers are found to be consistent with $J^{PC} = 0^{++}$, but small anomalous HVV couplings are still allowed. Such couplings are a subject of effective field theory (EFT) framework [31].

The HVV coupling measurements at the LHC have been performed using vector boson fusion (VBF), ZH, and WH production, and $H \to VV$ decays [11–30, 32]. However, the production of γH with an energetic photon recoiling against the H boson, similar to ZH production as shown in Fig. 1 (left), has not been directly studied at the LHC. A recent search for $WW\gamma$ production [33] was interpreted as a search for γH, where a relatively soft photon is produced as a radiative correction to quark-antiquark annihilation $q\bar{q} \to H$, as shown in Fig. 1 (right). Searches for heavy resonances decaying into a photon and a hadronically decaying H boson have been performed at the LHC [34–36]. Although the final-state topology in these searches resembles that of the processes of interest here, a direct interpretation within the EFT framework is not possible due to significant differences in the kinematic distributions, especially the photon energy spectrum, compared to those observed in the processes illustrated in Fig. 1.

The SM cross section of the associated photon and H boson production, $\sigma_{\gamma H}$, is expected to be less than 5 fb at the LHC [37] and is beyond the current experimental reach. However, new anomalous interactions may enhance such production, as discussed in Refs. [38–40]. The main production mechanisms are shown in Fig. 1 and the corresponding transverse momentum (p_T) spectra of the associated photons are shown in Fig. 2 [40–43]. The latter are important for assessing the feasibility of detecting such final states. In the case of bremsstrahlung radiation shown in Fig. 1 (right), the photon p_T spectrum is soft, a characteristic feature of quantum electrodynamics known as infrared divergence. In contrast, for Higgsstrahlung radiation shown in Fig. 1 (left), the coupling is induced by a loop-generated higher-dimensional operator that includes a momentum factor in the numerator. This factor cancels the divergent term in the denominator, leading to an energetic photon recoiling against the H boson. In this case, the photon p_T distribution peaks above 50 GeV and extends up to several hundred GeV, as shown in Fig. 2 [40].

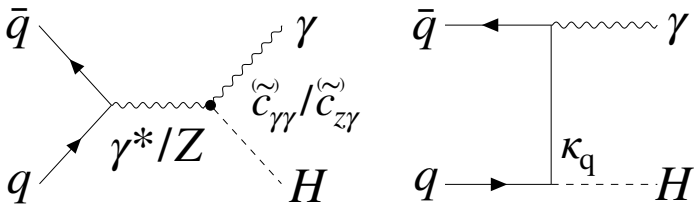

Figure 1: Examples of Feynman diagrams illustrating γH production at the LHC, highlighting the relevant couplings as discussed in the text. On the left, production occurs via an effective loop-generated $H\gamma\gamma$ or $HZ\gamma$ interaction, denoted by a dot, which is the primary focus of this paper. On the right, production proceeds through H boson production in $q\bar{q}$ annihilation with photon radiation.

The primary production mechanism targeted in this analysis is generated by the effective $HZ\gamma$ and $H\gamma\gamma$ vertices, as shown in Fig. 1 (left). The hard p_T spectrum resulting from anomalous $H\gamma\gamma$ or $HZ\gamma$ interactions makes it possible to distinguish such final states. These interactions

could be generated by heavy particles in the loops leading to both *CP*-even and *CP*-odd EFT operators, with Wilson coefficients $c_{\gamma\gamma}$, $c_{z\gamma}$, $\tilde{c}_{\gamma\gamma}$, and $\tilde{c}_{z\gamma}$ when expressed in the mass-eigenstate basis [31]. Each of these operators can be represented as a combination of three operators in the weak-eigenstate basis [31]. Overall, there are six operators to consider in the weak-eigenstate basis, with the Wilson coefficients $C^{\varphi W}$, $C^{\varphi B}$, $C^{\varphi WB}$, $C^{\varphi \tilde{W}}$, $C^{\varphi \tilde{B}}$, and $C^{\varphi \tilde{W}B}$. Because of the smaller number of operators, the mass-eigenstate basis is chosen for this result, which can then be translated into the weak-eigenstate basis.

The $qqH\gamma$ point interaction, shown in Fig. 3 (left), with the linear combination of Wilson coefficients C^{qB} and C^{qW}, equivalent to one coefficient $c_{q\gamma}$ in the mass eigenstate notation, can generate γH production in $q\bar{q}$ annihilation with a photon p_T spectrum even harder than that produced by anomalous $HV\gamma$ couplings, as shown in Fig. 2 [41–43]. The point interaction appears in the Feynman rules of the Standard Model Effective Field Theory (SMEFT) [44]. However, the same beyond-the-SM (BSM) operators also contribute to the $q\bar{q}\gamma$ interaction, shown in Fig. 3 (right), and $q\bar{q}Z$ interaction in the Feynman rules [44]. These operators are expected to be much better constrained by the more abundant processes without the presence of the H boson, such as Drell–Yan. Although a fully optimized analysis of the Drell–Yan process to target various Wilson coefficients has not yet been performed at the LHC, current theoretical interpretations of published $pp \to \ell\nu$ and $pp \to \ell\ell$ results at the LHC indicate that the current constraints on the C^{qB} and C^{qW} Wilson coefficients from Drell–Yan are significantly stronger than those from processes involving the H boson [45]. For these reasons, we do not consider this production diagram in this analysis.

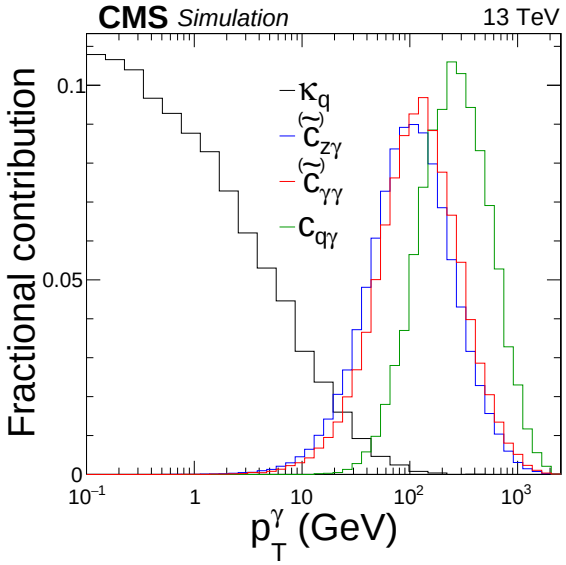

Figure 2: The spectrum of the photon transverse momentum in γH production, as generated by the leading-order diagrams shown in Figs. 1 and 3. The four distributions correspond to production resulting from couplings κ_q, $c_{z\gamma}$ ($\tilde{c}_{z\gamma}$), $c_{\gamma\gamma}$ ($\tilde{c}_{\gamma\gamma}$), and $c_{q\gamma}$.

The Yukawa couplings of quarks y_q are incorporated into the effective Lagrangian that describes their interaction with the H boson as

$$\mathcal{L}(Hq\bar{q}) = -y_q \bar{\psi}_q \psi_q H, \tag{1}$$

where $\bar{\psi}_q$ and ψ_q denote the Dirac spinors for a quark q, which can be u, d, s, c, b, or t. In the SM, $y_q^{SM} = m_q/v$, with $v = 246\,\text{GeV}$ being the vacuum expectation value of the Higgs field. The quark Yukawa couplings may also be expressed in two alternative forms. First, we

define $\kappa_q = y_q v/m_q$, which is useful because $\kappa_q^{SM} = 1$. Hence, κ_q may also be interpreted as the modifier for the coupling strength of the quark q to the H boson. Second, we define $\overline{\kappa}_q = y_q v/m_b$ [46], which is particularly useful for comparing the hierarchy of the Yukawa couplings of light quarks, with respect to $\overline{\kappa}_b^{SM} = 1$ for the down-type quarks or $\overline{\kappa}_t^{SM} = m_t/m_b$ for the up-type quarks. In these calculations, the quark masses are evaluated at the scale $\mu = 125\,\text{GeV}$, which are used to relate $\overline{\kappa}_q = \kappa_q m_q/m_b$.

The emission of the H boson and a photon from a quark in the $q\bar{q}$ annihilation, depicted in Fig. 1 (right), is the dominant γH production channel in the SM [37]. However, this production mechanism would result in a photon with very low p_T, of less than 1 GeV on average, as determined from a dedicated simulation shown in Fig. 2 [41–43]. Differentiating this production mechanism from others, such as gluon fusion (ggH), becomes exceedingly challenging because of the presence of soft photons, whether genuine or spurious, throughout the rest of the proton-proton (pp) collision event. Nevertheless, an increased Yukawa coupling of light quarks could change the production rate associated with this mechanism.

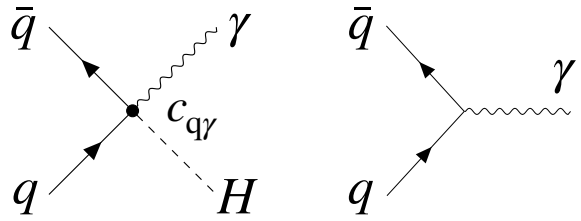

Figure 3: Feynman diagrams describing the $q\bar{q}$ annihilation with production of γH through a point-like EFT operator (left) and with photon production (right).

This motivated an approach to constrain the Yukawa coupling of light quarks by imposing constraints on the γH production rate [47]. However, the presence of an associated photon in this context does not effectively aid such an analysis due to the soft p_T spectrum. This photon merely represents a radiative correction to the direct $q\bar{q}$ annihilation illustrated in Fig. 4 (left). Therefore, we investigate the inclusive production of the H boson to explore the potential enhancement of the Hqq coupling. This enhancement would also change the rate of the gluon fusion process depicted in Fig. 4 (right), necessitating its consideration in this analysis as well. The concept for this analysis was initially introduced in Refs. [48, 49] and has been revisited more recently in Ref. [50].

Other strategies have been proposed to constrain the Yukawa couplings of bottom and charm quarks. Constraints on the Hcc coupling have been directly derived from searches for H boson decays into charm quarks [51, 52]. Measurements of transverse momentum distributions in H boson production [53] have been used to derive experimental constraints, as outlined in Refs. [54–56]. A proposal was made to constrain the charm Yukawa coupling through a global fit to the H boson signal strengths [57], although this approach overlooks the fact that SM assumptions are applied in these fits. Radiative decays of the H boson to mesons could also be used to constrain the quark couplings [58]. However, there are currently no stringent experimental constraints on the couplings involving the s, d, and u quarks. Nevertheless, it has been proposed that the transverse momentum and rapidity distributions of the H boson could help establish these constraints [59].

This paper is organized as follows. Section 2 provides a discussion of the CMS experiment and event reconstruction. Section 3 describes the modeling of signal and background processes. The selection of both $H \to 4\ell$ and $b\bar{b}$ events is presented in Section 4. Background estimation is discussed in Section 5, while the systematic uncertainties in the experimental measurement

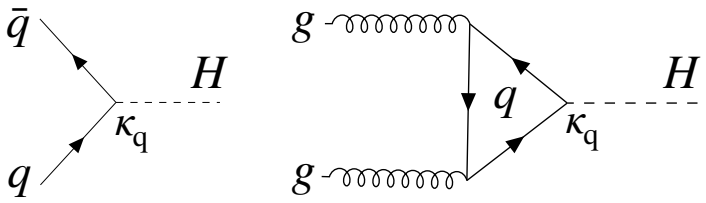

Figure 4: Feynman diagrams describing the H boson production at LHC through direct $q\bar{q}$ annihilation (left) and gluon fusion production (right).

of cross sections are outlined in Section 6. This is followed by a description of the two analyses in Sections 7 and 8, with a summary of both analyses provided in Section 9.

For the analysis described in Section 7, we follow the formalism and simulation tools from Ref. [40] and set upper limits on the γH production cross section, along with simultaneous constraints on four anomalous HZγ and H$\gamma\gamma$ couplings in the mass-eigenstate EFT basis. The analysis is based on the signature of an H boson boosted in the direction transverse to the beam and recoiling against a high-energy photon. Two final states in the decay of the H boson are considered: $\mathrm{H} \to \mathrm{b\bar{b}}$, with a branching fraction of $\mathcal{B}_{\mathrm{b\bar{b}}} = 0.577$, and $\mathrm{H} \to 4\ell$, with $\mathcal{B}_{4\ell} = 0.000128$, both evaluated at $m_{\mathrm{H}} = 125.38\,\mathrm{GeV}$ [31], where ℓ refers to either an electron or a muon. The boosted topology of the H boson gives preference to the former channel because of its much larger $\mathcal{B}$, but both channels are analyzed for completeness.

For the analysis in Section 8, we investigate the rate of H boson production for potential enhancements of the Yukawa couplings between light quarks and the H boson. This includes examining modifications to both direct quark-antiquark annihilation and gluon fusion loop processes. The enhanced Hqq couplings would lead to an increased width of the H boson and reduced rate of the on-shell process despite the increase of the amplitudes for the quark-antiquark annihilation and gluon fusion loop processes. The absence of significant changes in the SM rate imposes restrictions on the Yukawa couplings of light quarks. Some assumptions are required for this analysis. For instance, we assume that the Yukawa couplings for the bottom and top quarks take their SM values, and that the HVV coupling strength does not exceed its SM value. This analysis is conducted in the four-lepton decay channel because of its high purity, which enables inclusive reconstruction regardless of the H boson's production mechanism and kinematic properties.

Tabulated results are provided in the HEPData record for this analysis [60].

2 The CMS detector and event reconstruction

The central feature of the CMS apparatus is a superconducting solenoid of 6 m internal diameter, providing a magnetic field of 3.8 T. Within the solenoid volume are a silicon pixel and strip tracker, a lead tungstate crystal electromagnetic calorimeter (ECAL), and a brass and scintillator hadron calorimeter (HCAL), each composed of a barrel and two endcap sections. Forward calorimeters extend the pseudorapidity (η) coverage provided by the barrel and endcap detectors. Muons are measured in gas-ionization detectors embedded in the steel flux-return yoke outside the solenoid. A more detailed description of the CMS detector, together with a definition of the coordinate system used and the relevant kinematic variables, can be found in Ref. [61, 62].

The data from the CMS experiment at the LHC were recorded between 2016 and 2018, corresponding to an integrated luminosity of 138 fb^{-1} at a proton-proton center-of-mass collision

energy of 13 TeV. Events of interest were selected using a two-tier trigger system. The first level, composed of custom hardware processors, uses information from the calorimeters and muon detectors to select events at a rate of around 100 kHz within a fixed latency of about 4 μs [63]. The second level, known as the high-level trigger, consists of a farm of processors running a version of the full event reconstruction software optimized for fast processing, and reduces the event rate to around 1 kHz before data storage [64, 65].

The primary vertex is taken to be the vertex corresponding to the hardest scattering in the event, evaluated using tracking information alone, as described in Section 9.4.1 of Ref. [66].

A particle-flow algorithm [67] aims to reconstruct and identify each individual particle in an event, with an optimized combination of information from the various elements of the CMS detector. The energy of photons is obtained from the ECAL measurement. The energy of electrons is determined from a combination of the electron momentum at the primary interaction vertex as determined by the tracker, the energy of the corresponding ECAL cluster, and the energy sum of all bremsstrahlung photons spatially compatible with originating from the electron track. The energy of muons is obtained from the curvature of the corresponding track. The energy of charged hadrons is determined from a combination of their momentum measured in the tracker and the matching ECAL and HCAL energy deposits, corrected for the response function of the calorimeters to hadronic showers. Finally, the energy of neutral hadrons is obtained from the corresponding corrected ECAL and HCAL energies.

Jets are clustered from particle-flow candidates using the anti-k_T algorithm [68, 69] with a distance parameter of either 0.4 (AK4 jets) or 0.8 (AK8 jets). The jet momentum is defined as the vector sum of all particle momenta in a jet and is found from simulation to be, on average, within 5–10% of the true momentum over the entire p_T spectrum and detector acceptance [70].

3 Signal and background simulation

Simulated samples of signal and background events are produced using various Monte Carlo (MC) event generators, with the CMS detector response modeled by GEANT4 [71]. The effects of pileup are modeled assuming a total inelastic pp cross section of 69.2 mb [72]. All simulated event samples are weighted to match the distribution of the expected pileup profile of the data. The parton distribution functions (PDFs) used in this paper belong to the Neural Network Parton Distribution Functions (NNPDF) sets, versions 3.0 and 3.1 [73]. All MC samples are interfaced with PYTHIA 8.230 [74] for parton showering. The $H \to b\bar{b}$ decay is also simulated with PYTHIA.

The JHUGEN 7.5.2 [75–79] MC program is used to simulate the γH production at leading order (LO) in quantum chromodynamics (QCD) and electroweak interactions. The same program is used to simulate the $H \to 4\ell$ decay in all MC samples involving this final state. The MELA [75–79] package, which contains a library of matrix elements from JHUGEN for the H boson signal and MCFM 7.0.1 [80] for the 4ℓ background, is used for MC sample reweighting, and for optimal discriminant calculations. The γH samples are generated for various values of $c_{\gamma\gamma}$, $c_{z\gamma}$, $\tilde{c}_{\gamma\gamma}$, and $\tilde{c}_{z\gamma}$, and are reweighted to any hypothesis of interest. The production of the H boson through gluon fusion, VBF, in association with a Z or W boson, or with a $t\bar{t}$ pair is simulated using POWHEG v2 [81–85] at next-to-leading order (NLO) in QCD. Production in association with a $b\bar{b}$ pair or single top quark is simulated only at LO in QCD via JHUGEN. All SM cross sections of the H boson production processes are matched to the recommendation in Ref. [31]. There are no final-state photons in any of the SM processes for H boson production simulated at the matrix-element level. Therefore, the reconstructed photons in the SM simulation originate

either from genuine photons produced during parton showering and hadronization, or from other SM particles that satisfy the photon selection criteria.

The background in the $\mathrm{b\bar{b}}$ channel mostly consists of nonresonant QCD multijet production with a real or misidentified photon, as well as resonant $\mathrm{Z}+\gamma$ production. The $\mathrm{b\bar{b}}$ channel also makes use of a control event category that vetoes the presence of high-energy photons for which the QCD multijet, $\mathrm{W}+$jets, and $\mathrm{Z}+$jets processes are the significant contributions. The $\mathrm{W}+\gamma$ and $\mathrm{Z}+\gamma$ processes are modeled at NLO, while the rest are modeled at LO. All processes are generated using MADGRAPH5_aMC@NLO v2.4.2 [43].

The vector boson samples include boson decays to all flavors of quarks as well as up to three (four) extra partons at the matrix element level for $\mathrm{W}+$jets ($\mathrm{Z}+$jets) and up to one extra parton for $\mathrm{V}+\gamma$ samples. Jets from the matrix element calculation and the parton shower description are matched using the MLM prescription [86] for $\mathrm{V}+$jets samples and FXFX matching [87] for $\mathrm{V}+\gamma$ samples. Correction factors are applied to the $\mathrm{V}+$jets samples to match the generator-level p_{T} distributions with those predicted by the highest available order in the perturbative expansion. The QCD NLO corrections are derived using MADGRAPH5_aMC@NLO, simulating W and Z boson production with up to two additional partons and FXFX matching to the parton shower. The electroweak NLO corrections are taken from theoretical calculations in Ref. [88]. Electroweak NLO corrections, taken from Ref. [89], are also applied to the $\mathrm{Z}+\gamma$ sample.

In the 4ℓ channel, the main background, $\mathrm{q\bar{q}} \to \mathrm{ZZ}/\mathrm{Z}\gamma^{*} \to 4\ell$, is estimated from simulation with POWHEG at NLO in QCD. A fully differential cross section has been computed at next-to-next-to leading order (NNLO) in QCD [90], but it is not yet available in a parton-level event generator. Therefore the NNLO/NLO QCD correction is applied as a function of $m_{4\ell}$. The $\mathrm{gg} \to \mathrm{ZZ}/\mathrm{Z}\gamma^{*} \to 4\ell$ background and electroweak background production of 4ℓ are generated with the JHUGEN package, which relies on the MCFM matrix elements [91–93]. In order to include higher-order corrections, the *K* factors calculated for the H boson signal [31] are applied to these two background processes.

4 Event selection

Two mutually exclusive selection requirements are used in the $\mathrm{H} \to 4\ell$ and $\mathrm{b\bar{b}}$ channels. They are described in Sections 4.1 and 4.2, respectively. In both channels, two categories of events are selected. In one case, an H boson candidate is selected to be associated with a high-energy photon, and the category is called γ-tagged. The other selected events are assigned to the Untagged category.

4.1 Event selection in the four-lepton channel

The selection of 4ℓ events (H boson candidates) and associated photons closely follows the methods used in the earlier analyses [16, 17, 94, 95]. The main triggers select either a pair of electrons or muons, or an electron and a muon. The minimal p_{T} of the leading electron (muon) is 23 (17) GeV, while that of the subleading lepton is 12 (8) GeV. To maximize the signal acceptance, triggers requiring three leptons with lower p_{T} thresholds and no isolation requirement are also used, as are isolated single-electron and single-muon triggers with thresholds of 27 and 22 GeV in 2016, or 35 and 27 GeV in 2017 and 2018, respectively. The overall trigger efficiency for simulated signal events that pass the full selection chain of this analysis is larger than 99%. The trigger efficiency is measured in data using a sample of 4ℓ events collected by the single-lepton triggers and is found to be consistent with the expectation from simulation.

Electrons (muons) are reconstructed within the geometrical acceptance defined by a require-

ment on the pseudorapidity $|\eta| < 2.5\,(2.4)$ for $p_T > 7\,(5)$ GeV with an algorithm that combines information from the ECAL (muon system) and the tracker. A dedicated algorithm is used to collect the final-state radiation off leptons [94]. To distinguish leptons from prompt Z boson decays from those originating in hadron decays within jets, a lepton isolation requirement is applied in the analysis [94]. In addition, to suppress non-prompt and misidentified leptons, primary leptons are required to satisfy $|\text{SIP}| < 4$, where the significance of the impact parameter (SIP) is defined as $\text{SIP} = \text{IP}/\sigma_{\text{IP}}$. Here, IP refers to the lepton's three-dimensional impact parameter relative to the selected primary vertex, and σ_{IP} is its associated uncertainty.

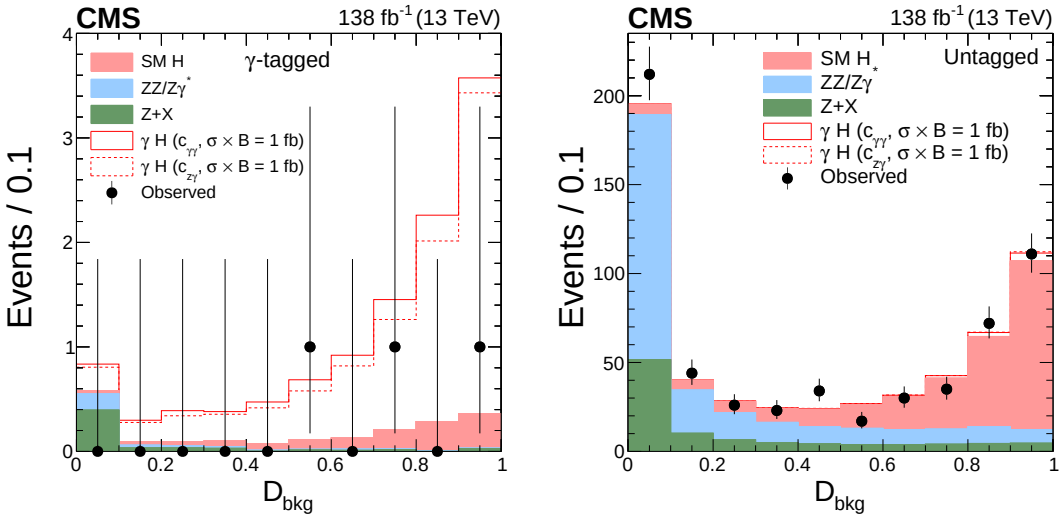

Figure 5: Distributions of events for the $\mathcal{D}_{\text{bkg}}$ observable in the γ-tagged (left) and Untagged (right) categories of the $H \to 4\ell$ candidate events. Observed events (black markers) and expected background estimates (solid histograms) from MC simulation ($ZZ/Z\gamma^*$) or control samples in data ($Z + X$) are shown. The γH signal contribution, stacked on top of background, is shown with an open histogram for an assumed cross section of $\sigma_{\gamma H}\,\mathcal{B}_{4\ell} = 1$ fb for either the $c_{\gamma\gamma}$ (solid) and $c_{z\gamma}$ (dashed) coupling hypothesis.

The γ-tagged category requires the presence of a photon passing loose cut-based identification requirements [96] and $p_T > 150$ GeV. All 4ℓ events that pass the selection requirements but do not include a photon that passes the requirements for the γ-tagged category enter the Untagged category. We consider three mutually exclusive channels: $H \to 4e$, 4μ, and $2e2\mu$. At least two leptons are required to have $p_T > 10$ GeV, and at least one is required to have $p_T > 20$ GeV. All four pairs of oppositely charged leptons that can be built with the four leptons are required to satisfy $m_{\ell^+\ell^-} > 4$ GeV regardless of lepton flavor. The Z boson candidates are required to satisfy the condition $12 < m_{\ell^+\ell^-} < 120$ GeV, where the invariant mass of at least one of the Z boson candidates must be larger than 40 GeV. The region between 105 and 140 GeV in the four-lepton invariant mass $m_{4\ell}$ is considered in this analysis.

Each event in the $H \to 4\ell$ channel is characterized by an optimal discriminant to separate signal from background. The discriminant is based on the H boson decay without using information related to the production mechanism, defined as

$$\mathcal{D}_{\text{bkg}}(\boldsymbol{\Omega}) = \frac{\mathcal{P}_{\text{sig}}(\boldsymbol{\Omega})}{\mathcal{P}_{\text{sig}}(\boldsymbol{\Omega}) + \mathcal{P}_{\text{bkg}}(\boldsymbol{\Omega})}, \tag{2}$$

where $\mathcal{P}_{\text{sig}}$ is the probability for the event to be consistent with the SM signal and $\mathcal{P}_{\text{bkg}}$ is the probability for the same event to be consistent with the dominant $q\bar{q} \to ZZ/Z\gamma^* \to 4\ell$

background. The probabilities $\mathcal{P}$ are calculated from the matrix elements provided by the MELA package using kinematic observables Ω, which are derived from the reconstructed momenta of the four leptons. These probabilities are normalized to give the same integrated cross sections in the relevant phase space of each process. Each matrix element probability is also multiplied by an empirical $m_{4\ell}$ parameterization, which includes resolution effects in the $m_{4\ell}$ distribution. The distributions of the $\mathcal{D}_{\text{bkg}}$ discriminant in the two categories of events are shown in Fig. 5.

4.2 Event selection in the $\mathrm{b\bar{b}}$ channel

In the $\mathrm{b\bar{b}}$ channel, the γ-tagged category aims to capture signal $\gamma\mathrm{H}$ events, while the Untagged category targets events with a boosted $\mathrm{Z} \to \mathrm{b\bar{b}}$ and a recoiling jet. The Untagged category also includes $\mathrm{H} \to \mathrm{b\bar{b}}$ events, although their contribution is negligible. The triggers in the γ-tagged category require events to have a photon with $p_{\mathrm{T}} > 175(200)$ GeV in 2016 (2017, 2018). The threshold is much lower than the p_{T} requirement placed in the offline selection described below. This makes the trigger selection almost fully efficient for the events that pass the offline selection.

The offline selection in the γ-tagged category requires that the leading p_{T} photon satisfies $p_{\mathrm{T}} > 300\,\text{GeV}$, $|\eta| < 2.4$, and the cut-based identification criteria at the tight working point [96]. An H boson candidate is defined as the AK8 jet with the highest p_{T} that also satisfies ΔR (jet, leading photon) > 0.8, where $\Delta R(1,2) \equiv \sqrt[htb]{(\eta_1-\eta_2)^2+(\varphi_1-\varphi_2)^2}$ is the distance between two objects in the pseudorapidity–azimuthal-angle plane. The H boson candidate is required to have $p_{\mathrm{T}} > 300\,\text{GeV}$ and $|\eta| < 2.4$. The analysis uses a mass decorrelated regression algorithm based on the PARTICLENET [97] graph convolutional neural network architecture to predict the jet mass M_{PNet} [98–100]. The H boson candidates are required to have the regressed mass $M_{\text{PNet}} > 60\,\text{GeV}$. A veto is placed on the presence of leptons, making the selected set of events orthogonal to that in the 4ℓ channel. To veto an event, a muon is required to have $p_{\mathrm{T}} > 20\,\text{GeV}$, $|\eta| < 2.4$, and must pass the loose identification and isolation criteria [101]. Similarly, a veto electron is required to have $p_{\mathrm{T}} > 20\,\text{GeV}$, $|\eta| < 2.4$, and must pass the cut-based identification at the veto working point [96]. Finally, a veto is placed on any b-tagged AK4 jet with $p_{\mathrm{T}} > 30\,\text{GeV}$ and $\Delta R(\text{jet, H candidate}) > 0.8$ in order to suppress the background arising from $\mathrm{t\bar{t}}$ production. The AK4 jets are identified as originating from b quarks using the DeepJet algorithm [102]. Events are classified based on how consistent the H boson candidate is with a boosted decay to $\mathrm{b\bar{b}}$, using the PARTICLENET algorithm, as described later in this section.

The Untagged category uses multiple triggers, based on energetic jet activity in the event, for the online selection. One trigger sets a requirement on the scalar p_{T} sum (H_{T}) of all AK4 jets. The H_{T} requirement is set to >800, >900, or >1050 GeV. A second trigger requires a presence of an AK8 jet with mass >30 GeV and $p_{\mathrm{T}} > 360$, 400, or 420 GeV. The third trigger condition is the presence of an AK8 jet with $p_{\mathrm{T}} > 450$ or 500 GeV. The final trigger requires $H_{\mathrm{T}} > 650$, 700, or 800 GeV together with an AK8 jet having a mass >50 GeV. The listed differing thresholds depend on the data-taking conditions with lower values typically being used in 2016. Events are selected if they pass any of the trigger conditions.

In the offline selection of the Untagged category, a Z boson candidate is defined as the AK8 jet with the highest p_{T}. It is required to satisfy $p_{\mathrm{T}} > 450\,\text{GeV}$, $M_{\text{PNet}} > 60\,\text{GeV}$, and $|\eta| < 2.4$. Conditions of $p_{\mathrm{T}} > 200\,\text{GeV}$ and $|\eta| < 2.4$ are also applied on the subleading (recoil) AK8 jet in order to further suppress the QCD multijet background. The Untagged category uses the same vetoes as the γ-tagged category. In addition, it places a veto on the presence of a photon with $p_{\mathrm{T}} > 300\,\text{GeV}$, making it orthogonal to the γ-tagged category.

The trigger efficiency of the Untagged event category is measured in data where online selec-

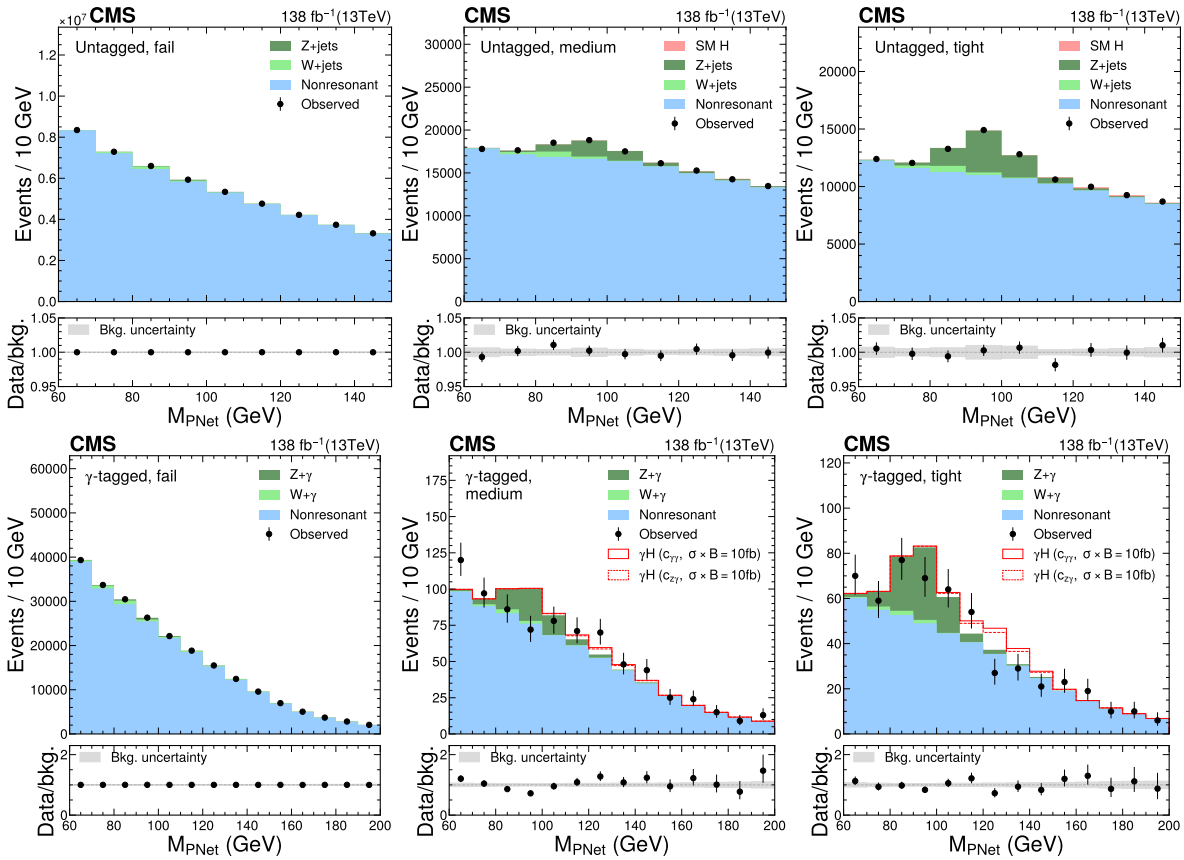

Figure 6: The M_{PNet} distributions for the number of observed events (black markers) compared with the backgrounds estimated in the fit to the data (filled histograms) in the $b\bar{b}$ channel. Fail (left), medium (middle) and tight (right) regions of the γ-tagged (lower) and Untagged (upper) categories are shown. The signal contribution, stacked on top of background, is shown with an open histogram for an assumed cross section of $\sigma_{\gamma H}\,\mathcal{B}_{b\bar{b}} = 10\,\text{fb}$.

tion requires an isolated muon with $p_T > 24\,\text{GeV}$ (27 GeV in 2017) or a muon with $p_T > 50\,\text{GeV}$ without any isolation requirements. The above offline selection is applied to these events in order to measure the trigger efficiency by counting the number of events satisfying the trigger selection. The trigger efficiency is expressed as a function of the Z boson p_T. It ranges from around 65% at 450 GeV and becomes fully efficient at 600 GeV. Simulated events are weighted by this efficiency as a function of the Z boson p_T and M_{PNet}.

The PARTICLENET architecture is also employed to discriminate the decays of a boosted massive particle X, which could be an H or a Z boson, to a pair of b quarks against a background of other jets, using the properties of the jet constituents as features. The multiclassifier PARTICLENET algorithm [97] outputs several variables, each in the range 0–1, and each of which can be interpreted as the probability of a jet having originated from a certain decay, such as from a massive resonance $X \to b\bar{b}$ ($P(X \to b\bar{b})$) or from a light-flavored quark or a gluon ($P(\text{QCD})$). In this analysis, the PARTICLENET score is defined as $P(X \to b\bar{b})/(P(X \to b\bar{b}) + P(\text{QCD}))$.

The PARTICLENET scores of the H and Z jets are used to classify events into mutually exclusive regions using high- and medium-purity working points [103]. If the candidate jet passes the high-purity working point, the event is sorted into the "tight" (T) region. If the candidate jet passes the medium-purity working point and fails the high-purity working point, the event is sorted into the "medium" (M) region. All other events are sorted into the "fail" (F) region.

To increase the channel sensitivity, the γ-tagged category is further split into two regions based on the photon p_T, 300–400 GeV and >400 GeV. This gives six regions in total in the γ-tagged category and three regions in the Untagged category. The distributions of the M_{PNet} observable, after fitting the background model to the data, are shown in Fig. 6 with the two p_T regions of the γ-tagged category combined. The background prediction mostly agrees with the data. The largest discrepancy is seen in the M region of the γ-tagged category where a deficit of events under the Z peak is observed. However, a goodness-of-fit test [104] confirmed the agreement between the data and the estimated background with the p-value [105] greater than 0.05, indicating no significant deviation.

5 Background estimation

5.1 Background estimation in the four-lepton channel

The dominant background to the $H \to 4\ell$ signal comes from $ZZ/Z\gamma^* \to 4\ell$ production in either $q\bar{q}$, gg, or electroweak processes. This background is estimated using the MC simulation discussed in Section 3. In addition, the $m_{4\ell}$ selection region between 105 and 140 GeV is wide enough to retain sideband regions for further constraints based on the data.

An additional background to the H boson signal, $Z + X$ in the following, comes from processes in which decays of heavy-flavor hadrons, decays of light mesons within jets, or charged hadrons overlapping with π^0 decays are misidentified as leptons. The main process contributing to these backgrounds is Z + jets, while subdominant processes in order of importance are $t\bar{t}$ + jets, $Z\gamma$ + jets, WZ + jets, and WW + jets. The $Z + X$ background is estimated from control regions in data. The control regions are defined as events that contain a lepton pair satisfying all the requirements of a Z candidate and two additional opposite-sign leptons where the two additional leptons satisfy identification requirements looser than those used in the analysis. These four leptons are then required to pass the H candidate selection. The yield in the signal region is obtained by weighting the control region events by the lepton misidentification probability, f_ℓ, defined as the fraction of nonsignal leptons that are identified by the analysis selection criteria. A detailed description of the method can be found in Ref. [94].

5.2 Background estimation in the $b\bar{b}$ channel

The $b\bar{b}$ channel is used to search for a narrow signal in the H boson candidate M_{PNet} distribution in the T and M regions of the γ-tagged category. The mass distributions in the γ-tagged category are split into two p_T regions (300–400 GeV and >400 GeV). Mass distributions of the nonresonant background are estimated using a pass-to-fail ratio method, described in the following paragraphs. The other relevant background processes in the γ-tagged category, $Z + \gamma$ and $W + \gamma$ are estimated from simulation. The simulated $Z + \gamma$ distributions are corrected by fitting the Z boson candidate M_{PNet} distributions to the data in the Untagged category. The nonresonant background is also estimated with the pass-to-fail ratio method in the Untagged category. The Z + jets and W + jets are estimated from simulation. Simulated distributions of the SM $H \to b\bar{b}$ process are also included in the Untagged category, but they have no significant impact on the results because of much lower yields compared to other processes.

The pass-to-fail ratio method is based on the ratio of M_{PNet} distributions between PARTICLENET passing (P = M or T) and failing regions. This gives two pass-to-fail ratios ($R_{P/F}$) per category. The $R_{M/F}(M_{PNet}, p_T)$, $R_{T/F}(M_{PNet}, p_T)$ in the γ-tagged category and $R^{0\gamma}_{M/F}(M_{PNet})$, $R^{0\gamma}_{T/F}(M_{PNet})$ in the Untagged category.

The nonresonant background, e.g., in the M region, is defined through the relation:

$$n_{\mathrm{M,nonres.}}(i) = n_{F,\mathrm{nonres.}}(i)\, R_{\mathrm{M/F}}(M_{\mathrm{PNet}}, p_{\mathrm{T}}), \tag{3}$$

where $n_{M(F),\mathrm{nonres.}}(i)$ is the number of nonresonant events in the i-th bin in the M (F) region. The F region is overwhelmingly dominated by nonresonant events, so $n_{\mathrm{F,nonres.}}(i)$ can be directly estimated from data by subtracting the relatively small simulated yields of other processes. The $R_{\mathrm{M/F}}$ is modeled as a polynomial in M_{PNet} and p_{T}. In the γ-tagged category, a polynomial of order n corresponds to a linear combination of $M_{\mathrm{PNet}}^{a} p_{\mathrm{T}}^{b}$ terms where $a + b \leq n$. Furthermore, since there are only two p_{T} regions, a condition $b < 2$ is imposed. In the Untagged category, a simple one-dimensional polynomial in M_{PNet} is used to model the corresponding ratio. The polynomial parameters are determined along with other likelihood parameters, while simultaneously fitting the model to the data across all regions. The above also applies to the estimate of nonresonant background in the T region.

A Fisher's F-test [106] on the unblinded fit to the data is used to determine the minimum polynomial order necessary and sufficient for the model. Starting from polynomials of order zero (constant $R_{\mathrm{P/F}}$), terms are added until no significant improvement is observed. The addition of terms is done independently for all four $R_{\mathrm{P/F}}$. The F-test shows that the first-order polynomial is preferred for each of the $R_{\mathrm{P/F}}$.

The prominent Z boson peak in the Untagged category is used to measure the PARTICLENET efficiency data-to-simulation scale factors. The two scale factors (T and M) are free parameters in the joint fit of γ-tagged and Untagged categories. They allow the migration of events from the T and M regions to the F region (and vice-versa), controlling the heights of the Z boson peak in both event categories. The scale factors are also applied to the signal γH process.

6 Systematic uncertainties

The measurement of the signal strength in this analysis is mainly affected by statistical uncertainties. Both experimental and theoretical systematic uncertainties that affect the shapes and the yields of the signals and backgrounds are incorporated in the likelihood as nuisance parameters [104]. The dominant theoretical uncertainties come from the QCD renormalization and factorization scales involved in the cross section computation. The uncertainties in the electroweak corrections on the cross sections, PDFs, and showering are also included.

Experimental uncertainties common to both the 4ℓ and $\mathrm{b\bar{b}}$ channels include uncertainties in the photon identification efficiency, as well as photon energy scale and resolution. The normalization of the signal and background processes derived from the MC simulation is affected by the uncertainty in the integrated luminosity [107–109].

When the Z + X background is estimated for the four-lepton channel, the flavor composition of QCD-evolved jets misidentified as leptons may be different in the $\mathrm{Z} + 1\ell$ and $\mathrm{Z} + 2\ell$ control regions, and together with the statistical uncertainty in the $\mathrm{Z} + 2\ell$ region, this uncertainty accounts for about a $\pm$30% variation in the Z + X background [95]. Uncertainties in the lepton momentum resolution and reconstruction efficiencies are small compared to other uncertainties.

In the $\mathrm{b\bar{b}}$ channel, the dominant experimental uncertainty comes from the PARTICLENET tagging efficiency, yielding an uncertainty in the γH signal normalization in the signal region of about 15% [103]. Other notable experimental uncertainties are those associated with the jet energy and mass corrections, and the trigger efficiency, affecting the signal yield by $<$1%.

Theoretical systematic uncertainties related to the analysis of light-quark Yukawa couplings are discussed in Section 8, along with the theoretical model of the H boson production cross section.

7 Results for γH cross section and HVV couplings

The cross section of the γH process, $\sigma_{\gamma H}$, is constrained in the $H \to b\bar{b}$ and 4ℓ channels. In both cases, a joint fit of the γH-tagged events and Untagged events is performed. The distribution of the M_{PNet} observable in the $b\bar{b}$ channel is shown in Fig. 6, and the distribution of the $\mathcal{D}_{\text{bkg}}$ observable in the 4ℓ channel is shown in Fig. 5. The two sets of distributions are shown after a joint fit to the data. No significant excess of γH events is visible in either channel.

The extended likelihood function is constructed using the probability densities describing the signal and background events as functions of the M_{PNet} and $\mathcal{D}_{\text{bkg}}$ observables in the $H \to b\bar{b}$ and 4ℓ channels, respectively. Simulation or control samples in data estimation are used to describe probability densities, as described in Sec. 5. The $\sigma_{\gamma H}$ is parameterized as a function of the couplings $c_{\gamma\gamma}$, $c_{z\gamma}$, $\tilde{c}_{\gamma\gamma}$, and $\tilde{c}_{z\gamma}$ [40], where the total width Γ_H of the H boson is assumed to have the SM value. It has been checked that Γ_H does not change significantly with variation of c_i within constraints obtained in this analysis, nor do kinematic distributions in the $H \to 4\ell$ decay, which can be assumed to be dominated by the SM tree-level coupling.

Table 1: Observed and expected constraints on the γH cross section $\sigma_{\gamma H}$ and on the $c_{\gamma\gamma}$, $c_{z\gamma}$, $\tilde{c}_{\gamma\gamma}$, and $\tilde{c}_{z\gamma}$ couplings using the $H \to b\bar{b}$ and 4ℓ channels combined. The third and fourth rows show constraints on cross section multiplied by the branching fraction using the $H \to b\bar{b}$ and $H \to 4\ell$ channels only, respectively. The 68% (central value with uncertainties) and 95% (upper limit or allowed intervals) CL intervals are shown.

Parameter	Scenario	Observed		Expected	
		68% CL	95% CL	68% CL	95% CL
$\sigma_{\gamma H}$ (fb)	$c_{z\gamma} = \tilde{c}_{z\gamma} = 0$	$-7.5^{+8.9}_{-8.8}$	<11.8	$0.0^{+6.3}_{-6.3}$	<16.1
$\sigma_{\gamma H}$ (fb)	float all	$-9.3^{+11.3}_{-11.2}$	<16.4	$0.0^{+8.0}_{-8.0}$	<21.5
$\sigma_{\gamma H}\,\mathcal{B}_{b\bar{b}}$ (fb)	float all	$-5.4^{+6.5}_{-6.5}$	<9.5	$0.0^{+4.6}_{-4.6}$	<12.4
$\sigma_{\gamma H}\,\mathcal{B}_{4\ell}$ (fb)	float all	$0.04^{+0.13}_{-0.04}$	<0.32	$0.00^{+0.08}_{-0.00}$	<0.32
$c_{\gamma\gamma}$	float all	0.00 ± 0.50	$[-0.84, 0.84]$	0.00 ± 0.63	$[-0.90, 0.90]$
$c_{\gamma\gamma}$	fix others	0.00 ± 0.46	$[-0.77, 0.77]$	0.00 ± 0.58	$[-0.83, 0.83]$
$c_{z\gamma}$	float all	0.00 ± 0.18	$[-0.30, 0.30]$	0.00 ± 0.22	$[-0.32, 0.32]$
$c_{z\gamma}$	fix others	0.00 ± 0.16	$[-0.27, 0.27]$	0.00 ± 0.21	$[-0.29, 0.29]$
$\tilde{c}_{\gamma\gamma}$	float all	0.00 ± 0.50	$[-0.84, 0.84]$	0.00 ± 0.63	$[-0.90, 0.90]$
$\tilde{c}_{\gamma\gamma}$	fix others	0.00 ± 0.46	$[-0.77, 0.77]$	0.00 ± 0.58	$[-0.83, 0.83]$
$\tilde{c}_{z\gamma}$	float all	0.00 ± 0.18	$[-0.30, 0.30]$	0.00 ± 0.22	$[-0.32, 0.32]$
$\tilde{c}_{z\gamma}$	fix others	0.00 ± 0.16	$[-0.27, 0.27]$	0.00 ± 0.21	$[-0.29, 0.29]$

The likelihood $\mathcal{L}$ is maximized with respect to the nuisance parameters, describing the systematic uncertainties, and the parameters of interest. There are four parameters of interest, which can either be the four anomalous couplings $c_{\gamma\gamma}$, $c_{z\gamma}$, $\tilde{c}_{\gamma\gamma}$, and $\tilde{c}_{z\gamma}$, or the cross-section $\sigma_{\gamma H}$ and three of the anomalous couplings, with the option to eliminate one of the couplings of choice.

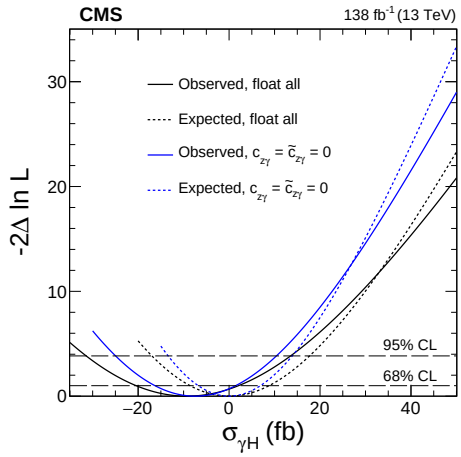

Figure 7: Constraints on $\sigma_{\gamma H}$ from the combination of the $H \to b\bar{b}$ and 4ℓ channels. The results are shown with only $c_{\gamma\gamma}$ and $\tilde{c}_{\gamma\gamma}$ floating in the fit (blue) and with all four couplings allowed to float (black). Observed (solid) and expected (dashed) likelihood scans are shown. The dashed horizontal lines show the 68 and 95% CL intervals.

Likelihood maximization is done using the Higgs COMBINE tool [104]. The allowed 68 and 95% confidence level (CL) intervals are defined using the profile likelihood function, $-2\Delta\mathcal{L} = 1.00$ and 3.84, for which exact coverage is expected in the asymptotic limit [110]. The 95% CL upper limits on $\sigma_{\gamma H}$ are determined with the requirement that cross sections must be positive. They are calculated using the CL_s criterion [111, 112] with the modified profiled likelihood ratio [110] as the test statistics.

Figure 7 shows the one-dimensional likelihood scan on $\sigma_{\gamma H}$ using the combination of the the $H \to b\bar{b}$ and 4ℓ channels. Due to the much larger branching fraction of the $H \to b\bar{b}$ channel, the combined results are dominated by these decays. Table 1 shows a summary of the 68 and 95% CL intervals on $\sigma_{\gamma H}$, either with no constraints on the couplings or allowing only the $c_{\gamma\gamma}$ and $\tilde{c}_{\gamma\gamma}$ couplings. The results for the $H \to 4\ell$ and $H \to b\bar{b}$ channels are presented separately with the cross section multiplied by the respective branching fraction. This highlights that, when the branching fraction is considered, the $H \to 4\ell$ channel is not competitive with the $H \to b\bar{b}$ channel. Negative cross sections are allowed, as indicated by the central values and 68% uncertainty ranges, except when setting the 95% CL upper limits on $\sigma_{\gamma H}$. In Fig. 7, the likelihood scan terminates for certain negative values of $\sigma_{\gamma H}$. This represents the case where some bins in the observables yield a negative number of events, so the total probability density function becomes negative for this extreme case.

Figure 8 shows the constraints on the squared couplings $c^2_{\gamma\gamma}$, $c^2_{z\gamma}$, $\tilde{c}^2_{\gamma\gamma}$, and $\tilde{c}^2_{z\gamma}$. Due to symmetry between the *CP*-even ($c^2_{\gamma\gamma}$ or $c^2_{z\gamma}$) and *CP*-odd ($\tilde{c}^2_{\gamma\gamma}$ or $\tilde{c}^2_{z\gamma}$) couplings, the likelihood scans projected on one dimension are indistinguishable, which is why only two graphs are displayed. We present constraints on the squared values because they are directly related to the event yields and most closely follow the Gaussian probability distributions. Table 1 shows a summary of the 68 and 95% CL intervals on four couplings, either with no constraints on the couplings or with certain couplings constrained to the null SM expectation.

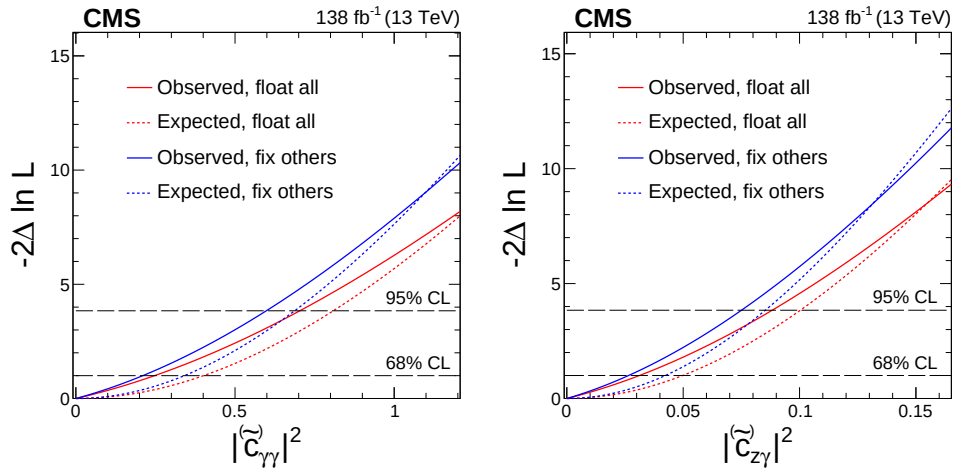

Figure 8: Constraints on the square of $|c_{\gamma\gamma}|$ (or $|\tilde{c}_{\gamma\gamma}|$) and $|c_{z\gamma}|$ (or $|\tilde{c}_{z\gamma}|$) from the combination of the $H \to b\bar{b}$ and 4ℓ channels. The other couplings are either fixed to the null SM expectation (blue) or are left floating in the fit (red). Observed (solid) and expected (dashed) likelihood scans are shown. The dashed horizontal lines show the 68 and 95% CL intervals.

8 Analysis of the light-quark Yukawa couplings

The limits on γH production could be used to constrain the Yukawa couplings of light quarks, as proposed in Ref. [47] and discussed in Section 1. However, the photon involved in this process is considerably softer than the one in diagram Fig. 1 (left). This motivates a reoptimization of the photon selection criteria introduced in Section 4.1. Upon testing, we find that the expected constraints remain unchanged, regardless of the selection requirement on p_T^γ. This effect is observed because a soft photon can easily be associated with an H boson produced via gluon fusion, for instance. Therefore, the distinction between the Untagged and γ-tagged categories is unnecessary. Instead, we must constrain light-quark Yukawa couplings by examining changes in the H boson production rate, regardless of the production mode.

This leads us to perform an inclusive analysis of $H \to 4\ell$ production, similar to the methods proposed in Refs. [48, 49], but with a more detailed focus on both the reconstruction and computational aspects. The four-lepton final state is especially suitable for this analysis because the decay is largely unaffected by the H boson couplings to quarks at the relevant scale. Additionally, the inclusive $H \to 4\ell$ reconstruction maintains high signal purity and is almost entirely independent of the production mechanism. Consequently, only the effects on production couplings and total width Γ_H of the H boson need to be taken into account. In this interpretation, we combine the Untagged and γ-tagged categories into one, while keeping the 4ℓ selection criteria unchanged.

8.1 Dependence of the cross sections on the light-quark Yukawa couplings

The SM $b\bar{b}H$ process serves as a reference for H boson production driven by light quarks at the tree level, $q\bar{q}H$, where the rates are adjusted according to κ_u, κ_d, κ_s, κ_c, and κ_b. The rate of the gluon fusion process is also expressed as a function of κ_q, while all other production mechanisms of the H boson considered remain unchanged. The couplings κ_b and κ_t are well constrained by the analysis of the on-shell H boson data [113, 114], including the $H \to b\bar{b}$ decay, and $t\bar{t}H$ and ggH production, and thus are fixed to $\kappa_b = \kappa_t = 1$ in this analysis. However, they are sometimes allowed to vary for studies and validation of the techniques presented in Section 8.2.

The total width of the H boson is parameterized, as shown below:

$$\Gamma_{\mathrm{H}} = R_{\mathrm{gg}}(\kappa_{\mathrm{u,d,s,c,b}})\,\Gamma^{\mathrm{SM}}_{\mathrm{H}\to\mathrm{gg}} + \sum_{\mathrm{q}=\mathrm{u,d,s,c,b}} \kappa^2_{\mathrm{q}}\,\Gamma^{\mathrm{SM}}_{\mathrm{H}\to\mathrm{q\bar{q}}} + \sum_{\mathrm{VV'}} \kappa^2_{\mathrm{VV'}}\,\Gamma^{\mathrm{SM}}_{\mathrm{H}\to\mathrm{VV'}} + \sum_{\ell}\Gamma^{\mathrm{SM}}_{\mathrm{H}\to\ell\ell} + \Gamma^{\mathrm{BSM}}_{\mathrm{H}}, \quad (4)$$

where the partial widths $\Gamma^{\mathrm{SM}}_{\mathrm{H}\to f}$ are calculated using the SM values for all couplings, while the partial width for decays to BSM particles is generally unknown and is constrained only by $\Gamma^{\mathrm{BSM}}_{\mathrm{H}} \geq 0$. In the partial width for the decay $\mathrm{H}\to\mathrm{VV'}$, V or V′ can be W, Z, or γ. Since this decay is primarily governed by the tree-level couplings HZZ and HWW, the influence of light-quark Yukawa couplings is highly suppressed and negligible compared to the direct $\mathrm{H}\to\mathrm{q\bar{q}}$ partial width with enhanced couplings. The coupling strength modifiers $\kappa_{\mathrm{VV'}}$ are introduced to account for potential BSM effects and will be elaborated on below. In the SM, their values are $\kappa_{\mathrm{VV'}} = 1$. The partial width for the decay $\mathrm{H}\to\ell\ell$, where ℓ denotes leptons e, μ, or τ, and neutrinos are neglected, is independent of κ_{q}. Thus, the dependence on κ_{q} is present only in the $\mathrm{H}\to\mathrm{q\bar{q}}$ and $\mathrm{H}\to\mathrm{gg}$ processes.

The cross section of the on-shell H boson production at the LHC, $\mathrm{pp}\to\mathrm{H}\to 4\ell$, is inversely proportional to the total width of the H boson and is parameterized as shown below:

$$\sigma_{\mathrm{H}\to 4\ell} = \frac{\Gamma^{\mathrm{SM}}_{\mathrm{H}\to 4\ell}\,\kappa^2_{\mathrm{ZZ}}}{\Gamma_{\mathrm{H}}(\kappa_{\mathrm{u,d,s,c,b}})}\left(R_{\mathrm{gg}}(\kappa_{\mathrm{u,d,s,c,b}})\,\sigma^{\mathrm{SM}}_{\mathrm{ggH}} + \sum_{\mathrm{q}}\kappa^2_{\mathrm{q}}\,\sigma^{\mathrm{SM}}_{\mathrm{q\bar{q}H}} + \sigma^{\mathrm{SM}}_{\mathrm{t\bar{t}H}} + \sigma^{\mathrm{SM}}_{\mathrm{tH}} + \sum_{\mathrm{VV}}\kappa^2_{\mathrm{VV}}\,\sigma^{\mathrm{SM}}_{\mathrm{VVH}}\right), \quad (5)$$

where the partial width for the decay $\mathrm{H}\to\mathrm{ZZ}\to 4\ell$, which is a subprocess of $\mathrm{H}\to\mathrm{ZZ}$, is scaled by the coupling strength modifier κ_{ZZ} introduced earlier, and all cross sections σ^{SM}_{i} are computed for the inclusive on-shell H boson production using the SM values for all couplings. The production in association with top quarks ($\mathrm{t\bar{t}H}$, tH) and VH or VBF production (VVH) are independent of κ_{q}. The latter arises for reasons similar to those discussed for the $\mathrm{H}\to\mathrm{VV'}$ decay, with some exceptions, such as the box diagram in the $\mathrm{gg}\to\mathrm{ZH}$ production. However, this contribution is minor in the $\mathrm{gg}\to\mathrm{ZH}$ process and is negligible compared to the $\mathrm{gg}\to\mathrm{H}$ process for any values of the quark Yukawa couplings. The VBF, ZH, and WH production processes are scaled by either κ^2_{ZZ} or κ^2_{WW}, with the interference between the two contributions in the VBF process being negligible.

The rates of the gluon fusion process in Eq. (5) and of the decay to gluons in Eq. (4) are both scaled by the same factor R_{gg}, which depends on the couplings of all quarks involved in the Hgg loop. The calculation of $R_{\mathrm{gg}}(\kappa_{\mathrm{u,d,s,c,b}})$ is carried out using MCFM code within the JHUGEN package, extending the computation in Ref. [40] to include light quarks. Since R_{gg} is used as a scaling factor in front of $\sigma^{\mathrm{SM}}_{\mathrm{ggH}}$ calculated at next-to-NNLO in QCD [31], the ggH cross section in Eq. (5) corresponds to the same order under the assumption that the K factor for matching the LO ggH cross section is independent of the quark flavor.

The partial decay width $\Gamma^{\mathrm{SM}}_{\mathrm{H}\to\mathrm{q\bar{q}}}$ in Eq. (4) is calculated using Ref. [115] for $\mathrm{q} = \mathrm{u,d,s,c}$, while the $\mathrm{H}\to\mathrm{b\bar{b}}$ value is obtained from Ref. [31]. The decay width of the H boson to two quarks is well understood under the assumption that the quark masses are small compared to the H boson mass $m_{\mathrm{H}} = 125\,\mathrm{GeV}$, which is a valid approximation for the light quarks considered in this analysis. Calculations use the running mass of the light quarks at m_{H} [116]. A uniform K factor is applied to match the $\mathrm{H}\to\mathrm{c\bar{c}}$ partial decay width to the most accurate value in Ref. [31].

Table 2: Central values of the input and derived parameters used in calculations involving Eqs. (4) and (5). The list of partons (p) comprises gluons (g) and five quark flavors (q). All cross sections σ_i are computed for the inclusive on-shell H boson production using the SM values for all couplings, except for the specific coupling κ_q that is explicitly mentioned.

p	$\Gamma^{SM}_{H\to p\bar{p}}/\Gamma^{SM}_{H}$	$\sigma^{SM}_{p\bar{p}H}$ (pb)	$\frac{\sigma_{ggH}(\kappa_q=0)}{\sigma^{SM}_{ggH}}-1$	$\frac{\sigma_{ggH}(\kappa_q\gg1)}{\sigma^{SM}_{ggH}}$	$\frac{\sigma_{q\bar{q}H}(\kappa_q\gg1)}{\sigma^{SM}_{ggH}}$
g	8.187×10^{-2}	4.858×10	—	—	—
b	5.824×10^{-1}	4.880×10^{-1}	1.595	1.422×10^{-2}	1.723×10^{-2}
c	2.891×10^{-2}	7.735×10^{-2}	4.254×10^{-2}	2.794×10^{-3}	5.506×10^{-2}
s	2.152×10^{-4}	1.854×10^{-3}	5.040×10^{-4}	1.518×10^{-4}	1.774×10^{-1}
d	5.552×10^{-7}	1.381×10^{-5}	2.087×10^{-6}	1.459×10^{-6}	5.120×10^{-1}
u	1.183×10^{-7}	4.155×10^{-6}	5.050×10^{-7}	4.189×10^{-7}	7.234×10^{-1}

The cross section of the $q\bar{q}H$ process as a function of the light-quark Yukawa coupling for each flavor of q in Eq. (5) is calculated at NNLO in QCD with SusHi [117]. As such, this process involves light quarks coupled to the H boson in either the initial or final states. Reference [118] demonstrated that the calculation for $b\bar{b}H$ at NNLO in QCD is analogous to the calculation for $q\bar{q}H$ production with light quarks. The main differences stem from the distinct quark Yukawa couplings and variations in the flavor composition of the PDFs. The central values for the QCD factorization and renormalization scales are set to $m_H/4$ and m_H, respectively, with systematic variations by a factor of 2, leading to cross section uncertainties between 3 and 5%, depending on the quark flavor. Similarly, PDF variations lead to uncertainties between 3 and 9%. For the $b\bar{b}H$ and $c\bar{c}H$ processes, the cross sections from Ref. [31] are reproduced with good accuracy. The typical K factor relative to the LO in the QCD calculation of the process $q\bar{q} \to H$ is 1.2. The effect of the interference between the $q\bar{q}H$ process and gluon fusion at higher orders in QCD is found to be negligible compared to the individual contributions.

Table 2 illustrates the numerical values of the parameters used in calculations involving Eqs. (4) and (5), as well as their asymptotic behavior. The concept of this analysis can be grasped by examining how the calculation in Eq. (5) varies with κ_q for a specific quark flavor q. Cross sections for all processes that do not explicitly depend on κ_q will decrease as κ_q increases above 1, due to the rise in $\Gamma_H(\kappa_q)$ in the denominator, as indicated by Eq. (4). The cross section for the gluon fusion process will also decrease, but at a slower rate due to the interplay between the quadratic dependence on κ_q in both the total width and R_{gg}. This cross section will ultimately reach a plateau at $\kappa_q \gg 1$ when the κ_q^2 term becomes dominant in $R_{gg}(\kappa_q)$. In contrast, the cross section for the $q\bar{q}H$ process will increase with rising κ_q because the numerator in Eq. (5) grows faster than the denominator. However, this increase will eventually level off, reaching an asymptotic value at $\kappa_q \gg 1$, where the terms proportional to κ_q^2 become dominant in both the numerator and the denominator.

8.2 Results for light-quark Yukawa couplings

This analysis is feasible because the total cross section for the $pp \to H \to 4\ell$ process decreases monotonically with increasing κ_q^2, eventually becoming inconsistent with the data and thus placing constraints on κ_q. Consequently, it is possible to simultaneously set constraints on the couplings of all four quark flavors $q = u, d, s, c$, without compromising precision, provided that the constraints are consistent with null measurements of these couplings. This occurs because, in the case of a null result for one coupling, introducing a non-zero value for another

coupling can only reduce the expected cross section, thereby tightening the constraint. Once the precision of these measurements is sufficient to detect significant nonzero values, distinguishing between the couplings will become challenging.

Incorporating BSM contributions, with Γ_H^{BSM} in Eq. (4) and κ_{ZZ} in Eq. (5), does not affect the upper limits, given the following two reasons. First, introducing a nonnegative Γ_H^{BSM} will further decrease the expected cross section, making its null value the most probable outcome when κ_q^2 is enhanced. Second, enforcing the assumption $\kappa_{ZZ}^2 \leq 1$ and $\kappa_{WW}^2 \leq 1$ in Eq. (5) is theoretically well-supported across various models [119]. This includes models with any number of Higgs doublets, both with and without additional Higgs singlets, as well as certain types of composite Higgs models.

Since all four $\kappa_{VV'}$ parameters must be taken into account in Eq. (4), we set $\kappa_{Z\gamma} = \kappa_{\gamma\gamma} = 1$, $\kappa_{ZZ} = \kappa_{WW}$, and $\kappa_{ZZ}^2 \leq 1$. With this assumption, it is apparent that allowing κ_{ZZ} to be a free parameter in Eq. (5) would result in $\kappa_{ZZ}^2 = 1$ being the most likely value when κ_q^2 is increased. It should be noted that technically the cross section σ_{tH}^{SM} in Eq. (5) also depends on κ_{WW}. However, this contribution is insufficient to counteract the reduction in other terms in Eq. (5) that results from a decrease in κ_{ZZ}^2.

Table 3: Observed and expected constraints on the κ_u, κ_d, κ_s, and κ_c couplings are shown using the $H \to 4\ell$ channel. In one scenario, all couplings except the one being shown are fixed at their SM values. In the other scenario, the Yukawa couplings for the three other light quarks are left unconstrained, and BSM contributions are allowed. The 68% (central value with error bars) and 95% (bracketed range or upper limit) CL intervals are displayed.

Parameter	Scenario	Observed		Expected	
		68% CL	95% CL	68% CL	95% CL
κ_u	float all	$(0.0 \pm 1.5) \times 10^3$	$[-2.4, 2.4] \times 10^3$	$(0.0 \pm 1.8) \times 10^3$	$[-2.6, 2.6] \times 10^3$
κ_u	fix others	$(0.0 \pm 1.4) \times 10^3$	$[-2.3, 2.3] \times 10^3$	$(0.0 \pm 1.6) \times 10^3$	$[-2.5, 2.5] \times 10^3$
κ_d	float all	$(0.0^{+6.7}_{-6.8}) \times 10^2$	$[-9.8, 9.8] \times 10^2$	$(0.0 \pm 7.4) \times 10^2$	$[-1.0, 1.0] \times 10^3$
κ_d	fix others	$(0.0^{+6.0}_{-6.0}) \times 10^2$	$[-9.4, 9.3] \times 10^2$	$(0.0^{+6.6}_{-6.7}) \times 10^2$	$[-9.9, 9.9] \times 10^2$
κ_s	float all	0^{+30}_{-32}	$[-44, 42]$	1^{+31}_{-32}	$[-44, 42]$
κ_s	fix others	0^{+27}_{-27}	$[-41, 40]$	1^{+27}_{-30}	$[-42, 40]$
κ_c	float all	$0.0^{+2.3}_{-2.8}$	$[-3.7, 3.2]$	$1.0^{+1.4}_{-3.8}$	$[-3.8, 3.3]$
κ_c	fix others	$0.9^{+1.4}_{-3.8}$	$[-3.8, 3.2]$	$1.0^{+1.4}_{-3.8}$	$[-3.9, 3.3]$
Γ_H^{BSM} (MeV)	float all	$0.0^{+0.7}_{-0.0}$	<1.4	$0.0^{+0.7}_{-0.0}$	<1.4

The fit to the data closely follows the approach outlined in Section 7. The extended likelihood function is built using probability densities that characterize both signal and background events as functions of the $\mathcal{D}_{bkg}$ observable in the 4ℓ channel. The $\mathcal{D}_{bkg}$ parameterizations for all $q\bar{q}H$ processes are modeled based on the $b\bar{b}H$ simulation, with the yields of all processes rescaled according to Eq. (5). The fit is conducted in two scenarios. In the first scenario, κ_q for a specific quark flavor q is left unconstrained, while all other coupling modifiers are fixed at their SM values: $\kappa_{q'} = 1$ for $q' \neq q$, $\kappa_{ZZ} = 1$, and $\Gamma_H^{BSM} = 0$. In the second scenario, $\kappa_b = \kappa_t = 1$ is set, while the Yukawa couplings of all other quarks remain unconstrained, with $\kappa_{ZZ}^2 \leq 1$ and $\Gamma_H^{BSM} \geq 0$. Figure 9 illustrates the constraints on each κ_q, and Table 3 presents the 68 and 95% CL intervals for κ_q in both scenarios. The results are quite similar in both scenarios, as previously discussed, but the results from the simultaneous fitting of all light-quark Yukawa

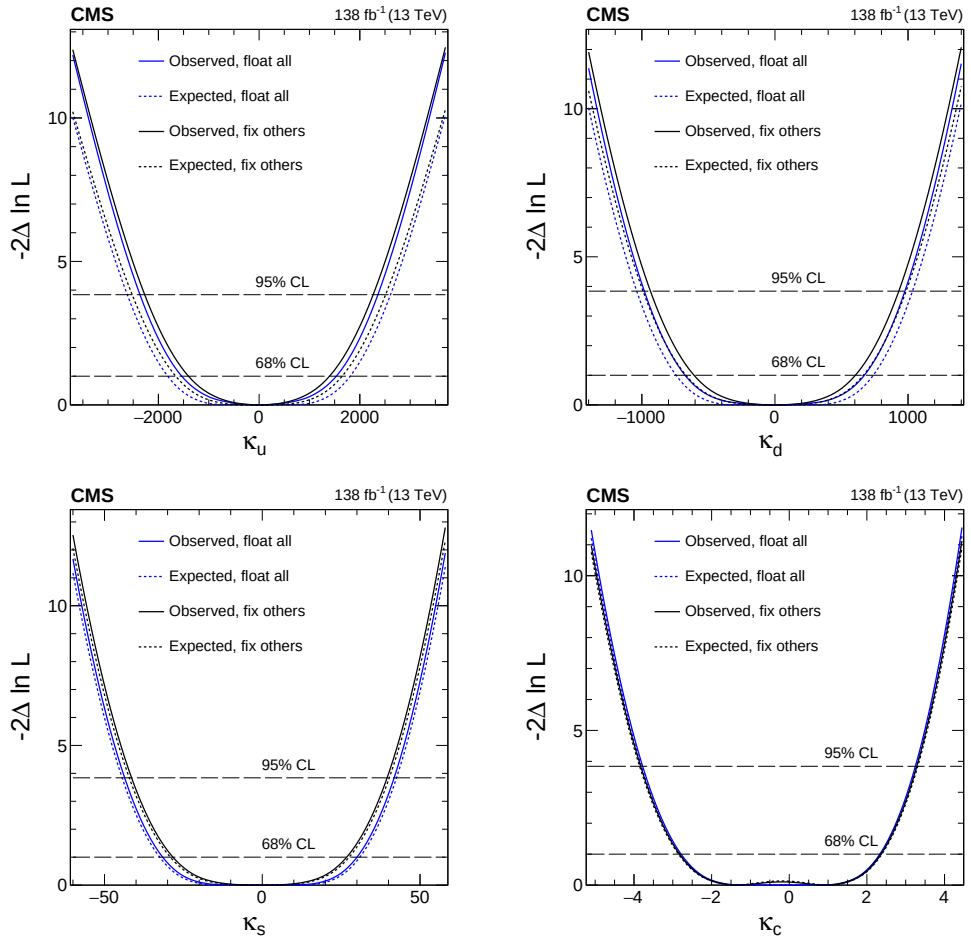

Figure 9: Constraints on κ_u, κ_d, κ_s, and κ_c are shown using the $H \to 4\ell$ channel. In scenario one (black), all couplings except the one being shown are fixed at their SM values. In scenario two (blue), the Yukawa couplings for the three other light quarks are left unconstrained, and BSM contributions are allowed: $\kappa^2_{ZZ} \leq 1$ and $\Gamma^{BSM}_H \geq 0$. Both observed (solid) and expected (dashed) constraints are presented. The crossings of dashed horizontal lines and the likelihood curves indicate the 68 and 95% CL intervals.

couplings are more general.

The results of the fit, represented by the $\overline{\kappa}_q$ parameters, provide a means to compare the hierarchy of Yukawa couplings of light quarks relative to the b and t quarks. These results are presented in Table 4. They are based on the assumption that both third-generation quarks, b and t, couple to the H boson with strengths consistent with the SM. Under this assumption, the hypothesis that $y_u = y_t^{SM}$, $y_c = y_t^{SM}$, $y_d = y_b^{SM}$, or $y_s = y_b^{SM}$, that is up-type (u or c) or down-type (d or s) quarks in the first or second generation, have the same couplings as those in the third generation (t or b, respectively), is excluded with a CL greater than 95%. It is not surprising that the limits on $\overline{\kappa}_q$ for the four light quarks are of a similar magnitude to the SM value for the b quark, as it is the Yukawa couplings that make a significant contribution to the H boson decay width.

When Γ^{BSM}_H is allowed to vary in the fit, the resulting constraints are: $\Gamma^{BSM}_H = 0.0^{+0.7}_{-0.0}$ MeV with an upper limit of 1.4 MeV at 95% CL. The constraints are expected to be $\Gamma^{BSM}_H = 0.0^{+0.7}_{-0.0}$ MeV (< 1.4 MeV). This constraint is possible due to the assumptions made about other couplings,

Table 4: Observed and expected constraints on the $\overline{\kappa}_u$, $\overline{\kappa}_d$, $\overline{\kappa}_s$, and $\overline{\kappa}_c$ defined as $\overline{\kappa}_q = y_q v/m_b$, following the same conventions as outlined in Table 3.

Parameter	Scenario	Observed		Expected	
		68% CL	95% CL	68% CL	95% CL
$\overline{\kappa}_u$	float all	0.00 ± 0.66	$[-1.02, 1.02]$	0.00 ± 0.79	$[-1.13, 1.13]$
$\overline{\kappa}_u$	fix others	$0.00^{+0.60}_{-0.61}$	$[-0.98, 0.98]$	$0.00^{+0.71}_{-0.72}$	$[-1.09, 1.09]$
$\overline{\kappa}_d$	float all	$0.00^{+0.63}_{-0.64}$	$[-0.93, 0.92]$	0.00 ± 0.70	$[-0.98, 0.97]$
$\overline{\kappa}_d$	fix others	0.00 ± 0.57	$[-0.88, 0.88]$	$0.00^{+0.63}_{-0.63}$	$[-0.93, 0.93]$
$\overline{\kappa}_s$	float all	$0.00^{+0.58}_{-0.60}$	$[-0.89, 0.85]$	$0.02^{+0.57}_{-0.64}$	$[-0.85, 0.81]$
$\overline{\kappa}_s$	fix others	$-0.01^{+0.52}_{-0.53}$	$[-0.79, 0.75]$	$0.02^{+0.51}_{-0.58}$	$[-0.81, 0.77]$
$\overline{\kappa}_c$	float all	$0.02^{+0.49}_{-0.63}$	$[-0.82, 0.71]$	$0.22^{+0.30}_{-0.84}$	$[-0.83, 0.72]$
$\overline{\kappa}_c$	fix others	$0.2^{+0.31}_{-0.83}$	$[-0.84, 0.72]$	$0.22^{+0.30}_{-0.85}$	$[-0.85, 0.73]$

such as $\kappa^2_{ZZ} < 1$. Bounds on Γ_H^{BSM} can be obtained from existing off-shell H boson data [20, 120, 121] without needing constraints on other couplings. However, these bounds, along with those obtained from the combined analysis of H boson data at the LHC [113, 114] are valid only under the assumption of small Yukawa couplings for the light quarks. This assumption is not applicable to the results presented in this paper.

In all of the fits mentioned above, the third-generation quark couplings are held fixed at their SM values, $\kappa_t = 1$ and $\kappa_b = 1$. If these constraints are relaxed to Gaussian constraints with 11 and 17% uncertainties, respectively, representing recent constraints from combined CMS data [114], the achieved bounds at 68% CL on κ_c, κ_s, κ_d, κ_u, and Γ_H^{BSM} vary by no more than 47, 37, 33, 33, and 95%, respectively. Alternatively, one can constrain only the top quark coupling, such as setting $\kappa_t = 1$, while allowing κ_b to vary freely, and still obtain bounds on the light-quark Yukawa couplings that are only somewhat less stringent than those shown in Table 3. For instance, a fit where κ_b and κ_c are allowed to vary would be analogous to the results presented in Eq. (12) and Fig. 27 (left) of Ref. [56] using the same $H \to 4\ell$ data, where only minor approximations were made compared to the methodology used in this paper.

9 Summary

A search for γH production is performed with the data from the CMS experiment at the LHC corresponding to an integrated luminosity of $138\,fb^{-1}$ at a proton-proton center-of-mass collision energy of 13 TeV. The analysis focuses on the topology of a boosted H boson recoiling against a high-energy photon. The final states of $H \to b\bar{b}$ and $H \to 4\ell$ are analyzed. This study examines effective $HZ\gamma$ and $H\gamma\gamma$ anomalous couplings within the context of an effective field theory. In this approach, the observed (expected) constraint on the γH production cross section is $\sigma_{\gamma H} < 16.4\,(21.5)$ fb at 95% CL. Simultaneous constraints on four anomalous couplings involving $HZ\gamma$ and $H\gamma\gamma$ are provided.

Additionally, the production rate for $H \to 4\ell$ is examined to assess potential enhancements in the Yukawa couplings between light quarks and the H boson. This includes examining modifications to both direct quark-antiquark annihilation and gluon fusion loop processes. Assuming the standard model Yukawa couplings for the bottom and top quarks ($\kappa_b = \kappa_t = 1$), along with the constraints on the HVV couplings ($\kappa^2_{WW} \leq 1$ and $\kappa^2_{ZZ} \leq 1$), the following simultaneous con-

straints are obtained: $\kappa_u = (0.0 \pm 1.5) \times 10^3$, $\kappa_d = (0.0^{+6.7}_{-6.8}) \times 10^2$, $\kappa_s = 0^{+30}_{-32}$, and $\kappa_c = 0.0^{+2.3}_{-2.8}$. The hypothesis that up- or down-type quarks in the first or second generation have the same Yukawa couplings as those in the third generation is excluded with a CL greater than 95%.

Acknowledgments

We congratulate our colleagues in the CERN accelerator departments for the excellent performance of the LHC and thank the technical and administrative staffs at CERN and at other CMS institutes for their contributions to the success of the CMS effort. In addition, we gratefully acknowledge the computing centers and personnel of the Worldwide LHC Computing Grid and other centers for delivering so effectively the computing infrastructure essential to our analyses. Finally, we acknowledge the enduring support for the construction and operation of the LHC, the CMS detector, and the supporting computing infrastructure provided by the following funding agencies: SC (Armenia), BMBWF and FWF (Austria); FNRS and FWO (Belgium); CNPq, CAPES, FAPERJ, FAPERGS, and FAPESP (Brazil); MES and BNSF (Bulgaria); CERN; CAS, MoST, and NSFC (China); MINCIENCIAS (Colombia); MSES and CSF (Croatia); RIF (Cyprus); SENESCYT (Ecuador); ERC PRG, RVTT3 and MoER TK202 (Estonia); Academy of Finland, MEC, and HIP (Finland); CEA and CNRS/IN2P3 (France); SRNSF (Georgia); BMBF, DFG, and HGF (Germany); GSRI (Greece); NKFIH (Hungary); DAE and DST (India); IPM (Iran); SFI (Ireland); INFN (Italy); MSIP and NRF (Republic of Korea); MES (Latvia); LMTLT (Lithuania); MOE and UM (Malaysia); BUAP, CINVESTAV, CONACYT, LNS, SEP, and UASLP-FAI (Mexico); MOS (Montenegro); MBIE (New Zealand); PAEC (Pakistan); MES and NSC (Poland); FCT (Portugal); MESTD (Serbia); MICIU/AEI and PCTI (Spain); MOSTR (Sri Lanka); Swiss Funding Agencies (Switzerland); MST (Taipei); MHESI and NSTDA (Thailand); TUBITAK and TENMAK (Turkey); NASU (Ukraine); STFC (United Kingdom); DOE and NSF (USA).

Individuals have received support from the Marie-Curie program and the European Research Council and Horizon 2020 Grant, contract Nos. 675440, 724704, 752730, 758316, 765710, 824093, 101115353, 101002207, and COST Action CA16108 (European Union); the Leventis Foundation; the Alfred P. Sloan Foundation; the Alexander von Humboldt Foundation; the Science Committee, project no. 22rl-037 (Armenia); the Fonds pour la Formation à la Recherche dans l'Industrie et dans l'Agriculture (FRIA-Belgium); the Beijing Municipal Science & Technology Commission, No. Z191100007219010 and Fundamental Research Funds for the Central Universities (China); the Ministry of Education, Youth and Sports (MEYS) of the Czech Republic; the Shota Rustaveli National Science Foundation, grant FR-22-985 (Georgia); the Deutsche Forschungsgemeinschaft (DFG), among others, under Germany's Excellence Strategy – EXC 2121 "Quantum Universe" – 390833306, and under project number 400140256 - GRK2497; the Hellenic Foundation for Research and Innovation (HFRI), Project Number 2288 (Greece); the Hungarian Academy of Sciences, the New National Excellence Program - ÚNKP, the NKFIH research grants K 131991, K 133046, K 138136, K 143460, K 143477, K 146913, K 146914, K 147048, 2020-2.2.1-ED-2021-00181, TKP2021-NKTA-64, and 2021-4.1.2-NEMZ_KI-2024-00036 (Hungary); the Council of Science and Industrial Research, India; ICSC – National Research Center for High Performance Computing, Big Data and Quantum Computing and FAIR – Future Artificial Intelligence Research, funded by the NextGenerationEU program (Italy); the Latvian Council of Science; the Ministry of Education and Science, project no. 2022/WK/14, and the National Science Center, contracts Opus 2021/41/B/ST2/01369 and 2021/43/B/ST2/01552 (Poland); the Fundação para a Ciência e a Tecnologia, grant CEECIND/01334/2018 (Portugal); the National Priorities Research Program by Qatar National Research Fund; MICIU/AEI/10.13039/501100011033, ERDF/EU, "European Union NextGenerationEU/PRTR",

and Programa Severo Ochoa del Principado de Asturias (Spain); the Chulalongkorn Academic into Its 2nd Century Project Advancement Project, and the National Science, Research and Innovation Fund via the Program Management Unit for Human Resources & Institutional Development, Research and Innovation, grant B39G670016 (Thailand); the Kavli Foundation; the Nvidia Corporation; the SuperMicro Corporation; the Welch Foundation, contract C-1845; and the Weston Havens Foundation (USA).

References

[1] ATLAS Collaboration, "Observation of a new particle in the search for the standard model Higgs boson with the ATLAS detector at the LHC", *Phys. Lett. B* **716** (2012) 1, doi:10.1016/j.physletb.2012.08.020, arXiv:1207.7214.

[2] CMS Collaboration, "Observation of a new boson at a mass of 125 GeV with the CMS experiment at the LHC", *Phys. Lett. B* **716** (2012) 30, doi:10.1016/j.physletb.2012.08.021, arXiv:1207.7235.

[3] CMS Collaboration, "Observation of a new boson with mass near 125 GeV in pp collisions at $\sqrt{s} = 7$ and 8 TeV", *JHEP* **06** (2013) 081, doi:10.1007/JHEP06(2013)081, arXiv:1303.4571.

[4] S. L. Glashow, "Partial-symmetries of weak interactions", *Nucl. Phys.* **22** (1961) 579, doi:10.1016/0029-5582(61)90469-2.

[5] F. Englert and R. Brout, "Broken symmetry and the mass of gauge vector mesons", *Phys. Rev. Lett.* **13** (1964) 321, doi:10.1103/PhysRevLett.13.321.

[6] P. W. Higgs, "Broken symmetries, massless particles and gauge fields", *Phys. Lett.* **12** (1964) 132, doi:10.1016/0031-9163(64)91136-9.

[7] P. W. Higgs, "Broken symmetries and the masses of gauge bosons", *Phys. Rev. Lett.* **13** (1964) 508, doi:10.1103/PhysRevLett.13.508.

[8] G. S. Guralnik, C. R. Hagen, and T. W. B. Kibble, "Global conservation laws and massless particles", *Phys. Rev. Lett.* **13** (1964) 585, doi:10.1103/PhysRevLett.13.585.

[9] S. Weinberg, "A model of leptons", *Phys. Rev. Lett.* **19** (1967) 1264, doi:10.1103/PhysRevLett.19.1264.

[10] A. Salam, "Weak and electromagnetic interactions", in *Elementary particle physics: relativistic groups and analyticity*, N. Svartholm, ed., p. 367. Almqvist & Wiksell, Stockholm, 1968. Proceedings of the eighth Nobel symposium.

[11] CMS Collaboration, "Study of the mass and spin-parity of the Higgs boson candidate via its decays to Z boson pairs", *Phys. Rev. Lett.* **110** (2013) 081803, doi:10.1103/PhysRevLett.110.081803, arXiv:1212.6639.

[12] CMS Collaboration, "Measurement of the properties of a Higgs boson in the four-lepton final state", *Phys. Rev. D* **89** (2014) 092007, doi:10.1103/PhysRevD.89.092007, arXiv:1312.5353.

[13] CMS Collaboration, "Constraints on the spin-parity and anomalous HVV couplings of the Higgs boson in proton collisions at 7 and 8 TeV", *Phys. Rev. D* **92** (2015) 012004, doi:10.1103/PhysRevD.92.012004, arXiv:1411.3441.

[14] CMS Collaboration, "Limits on the Higgs boson lifetime and width from its decay to four charged leptons", *Phys. Rev. D* **92** (2015) 072010, doi:10.1103/PhysRevD.92.072010, arXiv:1507.06656.

[15] CMS Collaboration, "Combined search for anomalous pseudoscalar HVV couplings in VH ($H \to b\bar{b}$) production and $H \to VV$ decay", *Phys. Lett. B* **759** (2016) 672, doi:10.1016/j.physletb.2016.06.004, arXiv:1602.04305.

[16] CMS Collaboration, "Constraints on anomalous Higgs boson couplings using production and decay information in the four-lepton final state", *Phys. Lett. B* **775** (2017) 1, doi:10.1016/j.physletb.2017.10.021, arXiv:1707.00541.

[17] CMS Collaboration, "Measurements of the Higgs boson width and anomalous HVV couplings from on-shell and off-shell production in the four-lepton final state", *Phys. Rev. D* **99** (2019) 112003, doi:10.1103/PhysRevD.99.112003, arXiv:1901.00174.

[18] CMS Collaboration, "Constraints on anomalous HVV couplings from the production of Higgs bosons decaying to τ lepton pairs", *Phys. Rev. D* **100** (2019) 112002, doi:10.1103/PhysRevD.100.112002, arXiv:1903.06973.

[19] CMS Collaboration, "Constraints on anomalous Higgs boson couplings to vector bosons and fermions in its production and decay using the four-lepton final state", *Phys. Rev. D* **104** (2021) 052004, doi:10.1103/PhysRevD.104.052004, arXiv:2104.12152.

[20] CMS Collaboration, "Measurement of the Higgs boson width and evidence of its off-shell contributions to ZZ production", *Nature Phys.* **18** (2022) 1329, doi:10.1038/s41567-022-01682-0, arXiv:2202.06923.

[21] CMS Collaboration, "Constraints on anomalous Higgs boson couplings to vector bosons and fermions from the production of Higgs bosons using the $\tau\tau$ final state", *Phys. Rev. D* **108** (2023) 032013, doi:10.1103/PhysRevD.108.032013, arXiv:2205.05120.

[22] ATLAS Collaboration, "Evidence for the spin-0 nature of the Higgs boson using ATLAS data", *Phys. Lett. B* **726** (2013) 120, doi:10.1016/j.physletb.2013.08.026, arXiv:1307.1432.

[23] ATLAS Collaboration, "Study of the spin and parity of the Higgs boson in diboson decays with the ATLAS detector", *Eur. Phys. J. C* **75** (2015) 476, doi:10.1140/epjc/s10052-015-3685-1, arXiv:1506.05669.

[24] ATLAS Collaboration, "Test of CP invariance in vector-boson fusion production of the Higgs boson using the Optimal Observable method in the ditau decay channel with the ATLAS detector", *Eur. Phys. J. C* **76** (2016) 658, doi:10.1140/epjc/s10052-016-4499-5, arXiv:1602.04516.

[25] ATLAS Collaboration, "Measurement of inclusive and differential cross sections in the $H \to ZZ^* \to 4\ell$ decay channel in pp collisions at $\sqrt{s} = 13$ TeV with the ATLAS detector", *JHEP* **10** (2017) 132, doi:10.1007/JHEP10(2017)132, arXiv:1708.02810.

[26] ATLAS Collaboration, "Measurement of the Higgs boson coupling properties in the $H \to ZZ^* \to 4\ell$ decay channel at $\sqrt{s} = 13$ TeV with the ATLAS detector", *JHEP* **03** (2018) 095, doi:10.1007/JHEP03(2018)095, arXiv:1712.02304.

[27] ATLAS Collaboration, "Measurements of Higgs boson properties in the diphoton decay channel with 36 fb^{-1} of pp collision data at $\sqrt{s} = 13$ TeV with the ATLAS detector", *Phys. Rev. D* **98** (2018) 052005, doi:10.1103/PhysRevD.98.052005, arXiv:1802.04146.

[28] ATLAS Collaboration, "Higgs boson production cross-section measurements and their EFT interpretation in the 4ℓ decay channel at $\sqrt{s} = 13$ TeV with the ATLAS detector", *Eur. Phys. J. C* **80** (2020) 957, doi:10.1140/epjc/s10052-020-8227-9, arXiv:2004.03447. [Erratum: doi:10.1140/epjc/s10052-021-09116-6].

[29] ATLAS Collaboration, "Test of CP invariance in Higgs boson vector-boson-fusion production using the $H \to \gamma\gamma$ channel with the ATLAS detector", *Phys. Rev. Lett.* **131** (2023) 061802, doi:10.1103/PhysRevLett.131.061802, arXiv:2208.02338.

[30] ATLAS Collaboration, "Test of CP-invariance of the Higgs boson in vector-boson fusion production and its decay into four leptons", *JHEP* **05** (2024) 105, doi:10.1007/JHEP05(2024)105, arXiv:2304.09612.

[31] D. de Florian et al., "Handbook of LHC Higgs cross sections: 4. deciphering the nature of the Higgs sector", CERN Report CERN-2017-002-M, 2016. doi:10.23731/CYRM-2017-002, arXiv:1610.07922.

[32] ATLAS and CMS Collaborations, "Evidence for the Higgs boson decay to a Z boson and a photon at the LHC", *Phys. Rev. Lett.* **132** (2024) 021803, doi:10.1103/PhysRevLett.132.021803, arXiv:2309.03501.

[33] CMS Collaboration, "Observation of WWγ production and search for Hγ production in proton-proton collisions at $\sqrt{s} = 13$ TeV", *Phys. Rev. Lett.* **132** (2024) 121901, doi:10.1103/PhysRevLett.132.121901, arXiv:2310.05164.

[34] CMS Collaboration, "Search for narrow Hγ resonances in proton-proton collisions at $\sqrt{s} = 13$ TeV", *Phys. Rev. Lett.* **122** (2019) 081804, doi:10.1103/PhysRevLett.122.081804, arXiv:1808.01257.

[35] ATLAS Collaboration, "Search for heavy resonances decaying to a photon and a hadronically decaying Z/W/H boson in pp collisions at $\sqrt{s} = 13$ TeV with the ATLAS detector", *Phys. Rev. D* **98** (2018) 032015, doi:10.1103/PhysRevD.98.032015, arXiv:1805.01908.

[36] ATLAS Collaboration, "Search for heavy resonances decaying into a photon and a hadronically decaying Higgs boson in pp collisions at $\sqrt{s} = 13$ TeV with the ATLAS detector", *Phys. Rev. Lett.* **125** (2020) 251802, doi:10.1103/PhysRevLett.125.251802, arXiv:2008.05928.

[37] A. Abbasabadi, D. Bowser-Chao, D. A. Dicus, and W. W. Repko, "Higgs-photon associated production at hadron colliders", *Phys. Rev. D* **58** (1998) 057301, doi:10.1103/PhysRevD.58.057301, arXiv:hep-ph/9706335.

[38] H. Khanpour, S. Khatibi, and M. M. Najafabadi, "Probing Higgs boson couplings in $H + \gamma$ production at the LHC", *Phys. Lett. B* **773** (2017) 462, doi:10.1016/j.physletb.2017.09.005, arXiv:1702.05753.

[39] L. Shi, Z. Liang, B. Liu, and Z. He, "Constraining the anomalous Higgs boson coupling in $H + \gamma$ production", *Chin. Phys. C* **43** (2019) 043001, doi:10.1088/1674-1137/43/4/043001, arXiv:1811.02261.

[40] J. Davis et al., "Constraining anomalous Higgs boson couplings to virtual photons", *Phys. Rev. D* **105** (2022) 096027, doi:10.1103/PhysRevD.105.096027, arXiv:2109.13363.

[41] I. Brivio, Y. Jiang, and M. Trott, "The SMEFTsim package, theory and tools", *JHEP* **12** (2017) 070, doi:10.1007/JHEP12(2017)070, arXiv:1709.06492.

[42] I. Brivio, "SMEFTsim 3.0 – a practical guide", *JHEP* **04** (2021) 073, doi:10.1007/JHEP04(2021)073, arXiv:2012.11343.

[43] J. Alwall et al., "The automated computation of tree-level and next-to-leading order differential cross sections, and their matching to parton shower simulations", *JHEP* **07** (2014) 079, doi:10.1007/jhep07(2014)079, arXiv:1405.0301.

[44] A. Dedes et al., "Feynman rules for the standard model effective field theory in R_ξ -gauges", *JHEP* **06** (2017) 143, doi:10.1007/JHEP06(2017)143, arXiv:1704.03888.

[45] ATLAS Collaboration, "Drell–Yan tails beyond the standard model", *JHEP* **03** (2023) 064, doi:10.1007/JHEP03(2023)064, arXiv:2207.10714v2.

[46] A. L. Kagan et al., "Exclusive window onto Higgs Yukawa couplings", *Phys. Rev. Lett.* **114** (2015) 101802, doi:10.1103/PhysRevLett.114.101802, arXiv:1406.1722.

[47] J. A. Aguilar-Saavedra, J. M. Cano, and J. M. No, "More light on Higgs flavor at the LHC: Higgs boson couplings to light quarks through $H + \gamma$ production", *Phys. Rev. D* **103** (2021) 095023, doi:10.1103/PhysRevD.103.095023, arXiv:2008.12538.

[48] Y. Zhou, "Constraining the Higgs boson coupling to light quarks in the $H \to ZZ$ final states", *Phys. Rev. D* **93** (2016) 013019, doi:10.1103/PhysRevD.93.013019, arXiv:1505.06369.

[49] Y. Zhou, "Probing anomalous couplings of the Higgs boson to weak bosons and fermions with precision calculations". PhD thesis, Johns Hopkins University, 2019. CERN-THESIS-2019-007.

[50] E. Balzani, R. Gröber, and M. Vitti, "Light-quark Yukawa couplings from off-shell Higgs production", *JHEP* **10** (2023) 027, doi:10.1007/JHEP10(2023)027, arXiv:2304.09772.

[51] CMS Collaboration, "Search for Higgs boson decay to a charm quark-antiquark pair in proton-proton collisions at $\sqrt{s} = 13$ TeV", *Phys. Rev. Lett.* **131** (2023) 061801, doi:10.1103/PhysRevLett.131.061801, arXiv:2205.05550.

[52] ATLAS Collaboration, "Direct constraint on the Higgs-charm coupling from a search for Higgs boson decays into charm quarks with the ATLAS detector", *Eur. Phys. J. C* **82** (2022) 717, doi:10.1140/epjc/s10052-022-10588-3, arXiv:2201.11428.

[53] F. Bishara, U. Haisch, P. F. Monni, and E. Re, "Constraining light-quark Yukawa couplings from Higgs distributions", *Phys. Rev. Lett.* **118** (2017) 121801, doi:10.1103/PhysRevLett.118.121801, arXiv:1606.09253.

[54] CMS Collaboration, "Measurement and interpretation of differential cross sections for Higgs boson production at $\sqrt{s} = 13$ TeV", *Phys. Lett. B* **792** (2019) 369, doi:10.1016/j.physletb.2019.03.059, arXiv:1812.06504.

[55] ATLAS Collaboration, "Measurement of the total and differential Higgs boson production cross-sections at $\sqrt{s} = 13\,\text{TeV}$ with the ATLAS detector by combining the $\text{H} \to \text{ZZ} \to 4\ell$ and $\text{H} \to \gamma\gamma$ decay channels", *JHEP* **05** (2023) 028, doi:10.1007/JHEP05(2023)028, arXiv:2207.08615.

[56] CMS Collaboration, "Measurements of inclusive and differential cross sections for the Higgs boson production and decay to four-leptons in proton-proton collisions at $\sqrt{s} = 13\,\text{TeV}$", *JHEP* **08** (2023) 040, doi:10.1007/JHEP08(2023)040, arXiv:2305.07532.

[57] G. Perez, Y. Soreq, E. Stamou, and K. Tobioka, "Constraining the charm Yukawa and Higgs-quark coupling universality", *Phys. Rev. D* **92** (2015), no. 3, 033016, doi:10.1103/PhysRevD.92.033016, arXiv:1503.00290.

[58] G. T. Bodwin, F. Petriello, S. Stoynev, and M. Velasco, "Higgs boson decays to quarkonia and the $\text{H}\bar{\text{c}}\text{c}$ coupling", *Phys. Rev. D* **88** (2013) 053003, doi:10.1103/PhysRevD.88.053003, arXiv:1306.5770.

[59] Y. Soreq, H. X. Zhu, and J. Zupan, "Light quark Yukawa couplings from Higgs kinematics", *JHEP* **12** (2016) 045, doi:10.1007/JHEP12(2016)045, arXiv:1606.09621.

[60] "HEPData record for this analysis", 2025. doi:10.17182/hepdata.154965.

[61] CMS Collaboration, "The CMS experiment at the CERN LHC", *JINST* **3** (2008) S08004, doi:10.1088/1748-0221/3/08/S08004.

[62] CMS Tracker Group Collaboration, "The CMS Phase-1 Pixel Detector Upgrade", *JINST* **16** (2021) P02027, doi:10.1088/1748-0221/16/02/P02027, arXiv:2012.14304.

[63] CMS Collaboration, "Performance of the CMS Level-1 trigger in proton-proton collisions at $\sqrt{s} = 13\,\text{TeV}$", *JINST* **15** (2020) P10017, doi:10.1088/1748-0221/15/10/P10017, arXiv:2006.10165.

[64] CMS Collaboration, "The CMS trigger system", *JINST* **12** (2017) P01020, doi:10.1088/1748-0221/12/01/P01020, arXiv:1609.02366.

[65] CMS Collaboration, "Performance of the CMS high-level trigger during LHC Run 2", *JINST* **19** (2024) P11021, doi:10.1088/1748-0221/19/11/P11021, arXiv:2410.17038.

[66] CMS Collaboration, "Technical proposal for the Phase-II upgrade of the Compact Muon Solenoid", CMS Technical Proposal CERN-LHCC-2015-010, CMS-TDR-15-02, 2015.

[67] CMS Collaboration, "Particle-flow reconstruction and global event description with the CMS detector", *JINST* **12** (2017) P10003, doi:10.1088/1748-0221/12/10/P10003, arXiv:1706.04965.

[68] M. Cacciari, G. P. Salam, and G. Soyez, "The anti-k_{T} jet clustering algorithm", *JHEP* **04** (2008) 063, doi:10.1088/1126-6708/2008/04/063, arXiv:0802.1189.

[69] M. Cacciari, G. P. Salam, and G. Soyez, "FastJet user manual", *Eur. Phys. J. C* **72** (2012) 1896, doi:10.1140/epjc/s10052-012-1896-2, arXiv:1111.6097.

[70] CMS Collaboration, "Jet energy scale and resolution in the CMS experiment in pp collisions at 8 TeV", *JINST* **12** (2017) P02014, doi:10.1088/1748-0221/12/02/P02014, arXiv:1607.03663.

[71] GEANT4 Collaboration, "GEANT4—a simulation toolkit", *Nucl. Instrum. Meth. A* **506** (2003) 250, doi:10.1016/S0168-9002(03)01368-8.

[72] CMS Collaboration, "Measurement of the inelastic proton-proton cross section at $\sqrt{s} = 13\,\text{TeV}$", *JHEP* **07** (2018) 161, doi:10.1007/JHEP07(2018)161, arXiv:1802.02613.

[73] NNPDF Collaboration, "Unbiased global determination of parton distributions and their uncertainties at NNLO and at LO", *Nucl. Phys. B* **855** (2012) 153, doi:10.1016/j.nuclphysb.2011.09.024, arXiv:1107.2652.

[74] T. Sjöstrand et al., "An introduction to PYTHIA 8.2", *Comput. Phys. Commun.* **191** (2015) 159, doi:10.1016/j.cpc.2015.01.024, arXiv:1410.3012.

[75] Y. Gao et al., "Spin determination of single-produced resonances at hadron colliders", *Phys. Rev. D* **81** (2010) 075022, doi:10.1103/PhysRevD.81.075022, arXiv:1001.3396.

[76] S. Bolognesi et al., "Spin and parity of a single-produced resonance at the LHC", *Phys. Rev. D* **86** (2012) 095031, doi:10.1103/PhysRevD.86.095031, arXiv:1208.4018.

[77] I. Anderson et al., "Constraining anomalous HVV interactions at proton and lepton colliders", *Phys. Rev. D* **89** (2014) 035007, doi:10.1103/PhysRevD.89.035007, arXiv:1309.4819.

[78] A. V. Gritsan, R. Röntsch, M. Schulze, and M. Xiao, "Constraining anomalous Higgs boson couplings to the heavy flavor fermions using matrix element techniques", *Phys. Rev. D* **94** (2016) 055023, doi:10.1103/PhysRevD.94.055023, arXiv:1606.03107.

[79] A. V. Gritsan et al., "New features in the JHU generator framework: constraining Higgs boson properties from on-shell and off-shell production", *Phys. Rev. D* **102** (2020) 056022, doi:10.1103/PhysRevD.102.056022, arXiv:2002.09888.

[80] J. M. Campbell and R. K. Ellis, "MCFM for the Tevatron and the LHC", *Nucl. Phys. Proc. Suppl.* **205-206** (2010) 10, doi:10.1016/j.nuclphysbps.2010.08.011, arXiv:1007.3492.

[81] S. Frixione, P. Nason, and C. Oleari, "Matching NLO QCD computations with parton shower simulations: the POWHEG method", *JHEP* **11** (2007) 070, doi:10.1088/1126-6708/2007/11/070, arXiv:0709.2092.

[82] E. Bagnaschi, G. Degrassi, P. Slavich, and A. Vicini, "Higgs production via gluon fusion in the POWHEG approach in the SM and in the MSSM", *JHEP* **02** (2012) 088, doi:10.1007/JHEP02(2012)088, arXiv:1111.2854.

[83] P. Nason and C. Oleari, "NLO Higgs boson production via vector-boson fusion matched with shower in POWHEG", *JHEP* **02** (2010) 037, doi:10.1007/JHEP02(2010)037, arXiv:0911.5299.

[84] G. Luisoni, P. Nason, C. Oleari, and F. Tramontano, "HW$^{\pm}$/HZ + 0 and 1 jet at NLO with the POWHEG BOX interfaced to GoSam and their merging within MiNLO", *JHEP* **10** (2013) 083, doi:10.1007/JHEP10(2013)083, arXiv:1306.2542.

[85] H. B. Hartanto, B. Jager, L. Reina, and D. Wackeroth, "Higgs boson production in association with top quarks in the POWHEG BOX", *Phys. Rev. D* **91** (2015) 094003, doi:10.1103/PhysRevD.91.094003, arXiv:1501.04498.

[86] J. Alwall et al., "Comparative study of various algorithms for the merging of parton showers and matrix elements in hadronic collisions", *Eur. Phys. J. C* **53** (2007) 473, doi:10.1140/epjc/s10052-007-0490-5, arXiv:0706.2569.

[87] R. Frederix and S. Frixione, "Merging meets matching in MC@NLO", *JHEP* **12** (2012) 061, doi:10.1007/JHEP12(2012)061, arXiv:1209.6215.

[88] J. M. Lindert et al., "Precise predictions for V+jets dark matter backgrounds", *Eur. Phys. J. C* **77** (2017) 829, doi:10.1140/epjc/s10052-017-5389-1, arXiv:1705.04664.

[89] A. Denner, S. Dittmaier, M. Hecht, and C. Pasold, "NLO QCD and electroweak corrections to Z+γ production with leptonic Z-boson decays", *JHEP* **02** (2016) 057, doi:10.1007/JHEP02(2016)057, arXiv:1510.08742.

[90] M. Grazzini, S. Kallweit, and D. Rathlev, "ZZ production at the LHC: fiducial cross sections and distributions in NNLO QCD", *Phys. Lett. B* **750** (2015) 407, doi:10.1016/j.physletb.2015.09.055, arXiv:1507.06257.

[91] J. M. Campbell, R. K. Ellis, and C. Williams, "Vector boson pair production at the LHC", *JHEP* **07** (2011) 018, doi:10.1007/JHEP07(2011)018, arXiv:1105.0020.

[92] J. M. Campbell, R. K. Ellis, and C. Williams, "Bounding the Higgs width at the LHC using full analytic results for gg $\to e^- e^+ \mu^- \mu^+$", *JHEP* **04** (2014) 060, doi:10.1007/JHEP04(2014)060, arXiv:1311.3589.

[93] J. M. Campbell and R. K. Ellis, "Higgs constraints from vector boson fusion and scattering", *JHEP* **04** (2015) 030, doi:10.1007/JHEP04(2015)030, arXiv:1502.02990.

[94] CMS Collaboration, "Measurements of properties of the Higgs boson decaying into the four-lepton final state in pp collisions at $\sqrt{s} = 13\,\text{TeV}$", *JHEP* **11** (2017) 047, doi:10.1007/JHEP11(2017)047, arXiv:1706.09936.

[95] CMS Collaboration, "Measurements of production cross sections of the Higgs boson in the four-lepton final state in proton proton collisions at $\sqrt{s} = 13\,\text{TeV}$", *Eur. Phys. J. C* **81** (2021) 488, doi:10.1140/epjc/s10052-021-09200-x, arXiv:2103.04956.

[96] CMS Collaboration, "Electron and photon reconstruction and identification with the CMS experiment at the CERN LHC", *JINST* **16** (2021) P05014, doi:10.1088/1748-0221/16/05/P05014, arXiv:2012.06888.

[97] H. Qu and L. Gouskos, "Jet tagging via particle clouds", *Phys. Rev. D* **101** (2020) 056019, doi:10.1103/PhysRevD.101.056019, arXiv:1902.08570.

[98] CMS Collaboration, "Mass regression of highly-boosted jets using graph neural networks", CMS Detector Performance Note CMS-DP-2021-017, 2021.

[99] CMS Collaboration, "Calibration of the mass-decorrelated ParticleNet tagger for boosted $b\bar{b}$ and $c\bar{c}$ jets using LHC Run 2 data", CMS Detector Performance Note CMS-DP-2022-005, 2022.

[100] CMS Collaboration, "Search for nonresonant pair production of highly energetic Higgs bosons decaying to bottom quarks", *Phys. Rev. Lett.* **131** (2023) 041803, doi:10.1103/PhysRevLett.131.041803, arXiv:2205.06667.

[101] CMS Collaboration, "Performance of the CMS muon detector and muon reconstruction with proton-proton collisions at $\sqrt{s} = 13$", *JINST* **13** (2018) P06015, doi:10.1088/1748-0221/13/06/P06015, arXiv:1804.04528.

[102] E. Bols et al., "Jet flavour classification using DeepJet", *JINST* **15** (2020) P12012, doi:10.1088/1748-0221/15/12/P12012, arXiv:2008.10519.

[103] CMS Collaboration, "Performance of heavy-flavour jet identification in boosted topologies in proton-proton collisions at $\sqrt{s} = 13$ TeV", 2025. arXiv:2510.10228. Submitted to JINST.

[104] CMS Collaboration, "The CMS statistical analysis and combination tool: COMBINE", *Comput. Softw. Big Sci.* **8** (2024) 19, doi:10.1007/s41781-024-00121-4, arXiv:2404.06614.

[105] L. Demortier, "P values and nuisance parameters", in *Statistical issues for LHC physics. Proceedings, Workshop, PHYSTAT-LHC, Geneva, Switzerland, June 27-29, 2007*, p. 23. 2008. doi:10.5170/CERN-2008-001.

[106] R. G. Lomax and D. L. Hahs-Vaughn, "Statistical concepts: a second course". Taylor and Francis, 2012.

[107] CMS Collaboration, "Precision luminosity measurement in proton-proton collisions at $\sqrt{s} = 13$ TeV in 2015 and 2016 at CMS", *Eur. Phys. J. C* **81** (2021) 800, doi:10.1140/epjc/s10052-021-09538-2, arXiv:2104.01927.

[108] CMS Collaboration, "CMS luminosity measurement for the 2017 data-taking period at $\sqrt{s}$ = 13 TeV", CMS Physics Analysis Summary CMS-PAS-LUM-17-004, 2018.

[109] CMS Collaboration, "CMS luminosity measurement for the 2018 data-taking period at $\sqrt{s}$ = 13 TeV", CMS Physics Analysis Summary CMS-PAS-LUM-18-002, 2019.

[110] G. Cowan, K. Cranmer, E. Gross, and O. Vitells, "Asymptotic formulae for likelihood-based tests of new physics", *Eur. Phys. J. C* **71** (2011) 1554, doi:10.1140/epjc/s10052-011-1554-0, arXiv:1007.1727. [Erratum: doi:10.1140/epjc/s10052-013-2501-z].

[111] T. Junk, "Confidence level computation for combining searches with small statistics", *Nucl. Instrum. Meth. A* **434** (1999) 435, doi:10.1016/S0168-9002(99)00498-2, arXiv:hep-ex/9902006.

[112] A. L. Read, "Presentation of search results: the CL_s technique", *J. Phys. G* **28** (2002) 2693, doi:10.1088/0954-3899/28/10/313.

[113] ATLAS Collaboration, "A detailed map of Higgs boson interactions by the ATLAS experiment ten years after the discovery", *Nature* **607** (2022) 52, doi:10.1038/10.1038/s41586-022-04893-w, arXiv:2207.00092. [Erratum: doi:10.1038/s41586-023-06248-5].

[114] CMS Collaboration, "A portrait of the Higgs boson by the CMS experiment ten years after the discovery", *Nature* **607** (2022) 60, doi:10.1038/s41586-022-04892-x, arXiv:2207.00043. [Erratum: doi:10.1038/s41586-023-06164-8].

[115] M. Spira, "QCD effects in Higgs physics", *Fortsch. Phys.* **46** (1998) 203, doi:10.1002/(SICI)1521-3978(199804)46:3<203::AID-PROP203>3.0.CO;2-4, arXiv:hep-ph/9705337.

[116] G.-y. Huang and S. Zhou, "Precise values of running quark and lepton masses in the standard model", *Phys. Rev. D* **103** (2021) 016010, doi:10.1103/PhysRevD.103.016010, arXiv:2009.04851.

[117] R. V. Harlander, S. Liebler, and H. Mantler, "SusHi: A program for the calculation of Higgs production in gluon fusion and bottom-quark annihilation in the standard model and the MSSM", *Comput. Phys. Commun.* **184** (2013) 1605, doi:10.1016/j.cpc.2013.02.006, arXiv:1212.3249.

[118] R. V. Harlander, "Higgs production in heavy quark annihilation through next-to-next-to-leading order QCD", *Eur. Phys. J. C* **76** (2016) 252, doi:10.1140/epjc/s10052-016-4093-x, arXiv:1512.04901.

[119] LHC Higgs Cross Section Working Group, "Handbook of LHC Higgs cross sections: 3. Higgs properties", *CERN Yellow Rep. Monogr.* **4** (2013) doi:10.5170/CERN-2013-004, arXiv:1307.1347.

[120] ATLAS Collaboration, "Evidence of off-shell Higgs boson production from ZZ leptonic decay channels and constraints on its total width with the ATLAS detector", *Phys. Lett. B* **846** (2023) 138223, doi:10.1016/j.physletb.2023.138223, arXiv:2304.01532.

[121] CMS Collaboration, "Measurement of the Higgs boson mass and width using the four-lepton final state in proton-proton collisions at 13 TeV", 2024. arXiv:2409.13663.

A The CMS Collaboration

Yerevan Physics Institute, Yerevan, Armenia
V. Chekhovsky, A. Hayrapetyan, V. Makarenko, A. Tumasyan[1]

Institut für Hochenergiephysik, Vienna, Austria
W. Adam, J.W. Andrejkovic, L. Benato, T. Bergauer, S. Chatterjee, K. Damanakis, M. Dragicevic, P.S. Hussain, M. Jeitler[2], N. Krammer, A. Li, D. Liko, I. Mikulec, J. Schieck[2], R. Schöfbeck[2], D. Schwarz, M. Sonawane, W. Waltenberger, C.-E. Wulz[2]

Universiteit Antwerpen, Antwerpen, Belgium
T. Janssen, H. Kwon, T. Van Laer, P. Van Mechelen

Vrije Universiteit Brussel, Brussel, Belgium
N. Breugelmans, J. D'Hondt, S. Dansana, A. De Moor, M. Delcourt, F. Heyen, Y. Hong, S. Lowette, I. Makarenko, D. Müller, S. Tavernier, M. Tytgat[3], G.P. Van Onsem, S. Van Putte, D. Vannerom

Université Libre de Bruxelles, Bruxelles, Belgium
B. Bilin, B. Clerbaux, A.K. Das, I. De Bruyn, G. De Lentdecker, H. Evard, L. Favart, P. Gianneios, A. Khalilzadeh, F.A. Khan, K. Lee, A. Malara, M.A. Shahzad, L. Thomas, M. Vanden Bemden, C. Vander Velde, P. Vanlaer

Ghent University, Ghent, Belgium
M. De Coen, D. Dobur, G. Gokbulut, J. Knolle, L. Lambrecht, D. Marckx, K. Skovpen, N. Van Den Bossche, J. van der Linden, J. Vandenbroeck, L. Wezenbeek

Université Catholique de Louvain, Louvain-la-Neuve, Belgium
S. Bein, A. Benecke, A. Bethani, G. Bruno, C. Caputo, J. De Favereau De Jeneret, C. Delaere, I.S. Donertas, A. Giammanco, A.O. Guzel, Sa. Jain, V. Lemaitre, J. Lidrych, P. Mastrapasqua, T.T. Tran, S. Turkcapar

Centro Brasileiro de Pesquisas Fisicas, Rio de Janeiro, Brazil
G.A. Alves, E. Coelho, G. Correia Silva, C. Hensel, T. Menezes De Oliveira, C. Mora Herrera[4], P. Rebello Teles, M. Soeiro, E.J. Tonelli Manganote[5], A. Vilela Pereira[4]

Universidade do Estado do Rio de Janeiro, Rio de Janeiro, Brazil
W.L. Aldá Júnior, M. Barroso Ferreira Filho, H. Brandao Malbouisson, W. Carvalho, J. Chinellato[6], E.M. Da Costa, G.G. Da Silveira[7], D. De Jesus Damiao, S. Fonseca De Souza, R. Gomes De Souza, T. Laux Kuhn[7], M. Macedo, J. Martins, K. Mota Amarilo, L. Mundim, H. Nogima, J.P. Pinheiro, A. Santoro, A. Sznajder, M. Thiel

Universidade Estadual Paulista, Universidade Federal do ABC, São Paulo, Brazil
C.A. Bernardes[7], L. Calligaris, T.R. Fernandez Perez Tomei, E.M. Gregores, I. Maietto Silverio, P.G. Mercadante, S.F. Novaes, B. Orzari, Sandra S. Padula, V. Scheurer

Institute for Nuclear Research and Nuclear Energy, Bulgarian Academy of Sciences, Sofia, Bulgaria
A. Aleksandrov, G. Antchev, R. Hadjiiska, P. Iaydjiev, M. Misheva, M. Shopova, G. Sultanov

University of Sofia, Sofia, Bulgaria
A. Dimitrov, L. Litov, B. Pavlov, P. Petkov, A. Petrov, E. Shumka

Instituto De Alta Investigación, Universidad de Tarapacá, Casilla 7 D, Arica, Chile
S. Keshri, D. Laroze, S. Thakur

Beihang University, Beijing, China
T. Cheng, T. Javaid, L. Yuan

Department of Physics, Tsinghua University, Beijing, China
Z. Hu, Z. Liang, J. Liu

Institute of High Energy Physics, Beijing, China
G.M. Chen[8], H.S. Chen[8], M. Chen[8], F. Iemmi, C.H. Jiang, A. Kapoor[9], H. Liao, Z.-A. Liu[10], R. Sharma[11], J.N. Song[10], J. Tao, C. Wang[8], J. Wang, Z. Wang[8], H. Zhang, J. Zhao

State Key Laboratory of Nuclear Physics and Technology, Peking University, Beijing, China
A. Agapitos, Y. Ban, A. Carvalho Antunes De Oliveira, S. Deng, B. Guo, C. Jiang, A. Levin, C. Li, Q. Li, Y. Mao, S. Qian, S.J. Qian, X. Qin, X. Sun, D. Wang, H. Yang, Y. Zhao, C. Zhou

Guangdong Provincial Key Laboratory of Nuclear Science and Guangdong-Hong Kong Joint Laboratory of Quantum Matter, South China Normal University, Guangzhou, China
S. Yang

Sun Yat-Sen University, Guangzhou, China
Z. You

University of Science and Technology of China, Hefei, China
K. Jaffel, N. Lu

Nanjing Normal University, Nanjing, China
G. Bauer[12], B. Li[13], H. Wang, K. Yi[14], J. Zhang

Institute of Modern Physics and Key Laboratory of Nuclear Physics and Ion-beam Application (MOE) - Fudan University, Shanghai, China
Y. Li

Zhejiang University, Hangzhou, Zhejiang, China
Z. Lin, C. Lu, M. Xiao

Universidad de Los Andes, Bogota, Colombia
C. Avila, D.A. Barbosa Trujillo, A. Cabrera, C. Florez, J. Fraga, J.A. Reyes Vega

Universidad de Antioquia, Medellin, Colombia
J. Jaramillo, C. Rendón, M. Rodriguez, A.A. Ruales Barbosa, J.D. Ruiz Alvarez

University of Split, Faculty of Electrical Engineering, Mechanical Engineering and Naval Architecture, Split, Croatia
D. Giljanovic, N. Godinovic, D. Lelas, A. Sculac

University of Split, Faculty of Science, Split, Croatia
M. Kovac, A. Petkovic, T. Sculac

Institute Rudjer Boskovic, Zagreb, Croatia
P. Bargassa, V. Brigljevic, B.K. Chitroda, D. Ferencek, K. Jakovcic, A. Starodumov[15],

T. Susa

University of Cyprus, Nicosia, Cyprus
A. Attikis, K. Christoforou, A. Hadjiagapiou, C. Leonidou, J. Mousa, C. Nicolaou, L. Paizanos, F. Ptochos, P.A. Razis, H. Rykaczewski, H. Saka, A. Stepennov

Charles University, Prague, Czech Republic
M. Finger, M. Finger Jr., A. Kveton

Universidad San Francisco de Quito, Quito, Ecuador
E. Carrera Jarrin

Academy of Scientific Research and Technology of the Arab Republic of Egypt, Egyptian Network of High Energy Physics, Cairo, Egypt
B. El-mahdy, S. Khalil[16], E. Salama[17,18]

Center for High Energy Physics (CHEP-FU), Fayoum University, El-Fayoum, Egypt
M. Abdullah Al-Mashad, M.A. Mahmoud

National Institute of Chemical Physics and Biophysics, Tallinn, Estonia
K. Ehataht, M. Kadastik, T. Lange, C. Nielsen, J. Pata, M. Raidal, L. Tani, C. Veelken

Department of Physics, University of Helsinki, Helsinki, Finland
K. Osterberg, M. Voutilainen

Helsinki Institute of Physics, Helsinki, Finland
N. Bin Norjoharuddeen, E. Brücken, F. Garcia, P. Inkaew, K.T.S. Kallonen, T. Lampén, K. Lassila-Perini, S. Lehti, T. Lindén, M. Myllymäki, M.m. Rantanen, J. Tuominiemi

Lappeenranta-Lahti University of Technology, Lappeenranta, Finland
H. Kirschenmann, P. Luukka, H. Petrow

IRFU, CEA, Université Paris-Saclay, Gif-sur-Yvette, France
M. Besancon, F. Couderc, M. Dejardin, D. Denegri, J.L. Faure, F. Ferri, S. Ganjour, P. Gras, G. Hamel de Monchenault, M. Kumar, V. Lohezic, J. Malcles, F. Orlandi, L. Portales, A. Rosowsky, M.Ö. Sahin, A. Savoy-Navarro[19], P. Simkina, M. Titov, M. Tornago

Laboratoire Leprince-Ringuet, CNRS/IN2P3, Ecole Polytechnique, Institut Polytechnique de Paris, Palaiseau, France
F. Beaudette, G. Boldrini, P. Busson, A. Cappati, C. Charlot, M. Chiusi, T.D. Cuisset, F. Damas, O. Davignon, A. De Wit, I.T. Ehle, B.A. Fontana Santos Alves, S. Ghosh, A. Gilbert, R. Granier de Cassagnac, A. Hakimi, B. Harikrishnan, L. Kalipoliti, G. Liu, M. Nguyen, S. Obraztsov, C. Ochando, R. Salerno, J.B. Sauvan, Y. Sirois, G. Sokmen, L. Urda Gómez, E. Vernazza, A. Zabi, A. Zghiche

Université de Strasbourg, CNRS, IPHC UMR 7178, Strasbourg, France
J.-L. Agram[20], J. Andrea, D. Apparu, D. Bloch, J.-M. Brom, E.C. Chabert, C. Collard, S. Falke, U. Goerlach, R. Haeberle, A.-C. Le Bihan, M. Meena, O. Poncet, G. Saha, M.A. Sessini, P. Van Hove, P. Vaucelle

Centre de Calcul de l'Institut National de Physique Nucleaire et de Physique des Particules, CNRS/IN2P3, Villeurbanne, France

A. Di Florio

Institut de Physique des 2 Infinis de Lyon (IP2I), Villeurbanne, France
D. Amram, S. Beauceron, B. Blancon, G. Boudoul, N. Chanon, D. Contardo, P. Depasse, C. Dozen[21], H. El Mamouni, J. Fay, S. Gascon, M. Gouzevitch, C. Greenberg, G. Grenier, B. Ille, E. Jourd'huy, M. Lethuillier, L. Mirabito, S. Perries, A. Purohit, M. Vander Donckt, P. Verdier, J. Xiao

Georgian Technical University, Tbilisi, Georgia
I. Lomidze, T. Toriashvili[22], Z. Tsamalaidze[15]

RWTH Aachen University, I. Physikalisches Institut, Aachen, Germany
V. Botta, S. Consuegra Rodríguez, L. Feld, K. Klein, M. Lipinski, D. Meuser, A. Pauls, D. Pérez Adán, N. Röwert, M. Teroerde

RWTH Aachen University, III. Physikalisches Institut A, Aachen, Germany
S. Diekmann, A. Dodonova, N. Eich, D. Eliseev, F. Engelke, J. Erdmann, M. Erdmann, B. Fischer, T. Hebbeker, K. Hoepfner, F. Ivone, A. Jung, M.y. Lee, F. Mausolf, M. Merschmeyer, A. Meyer, S. Mukherjee, D. Noll, F. Nowotny, A. Pozdnyakov, Y. Rath, W. Redjeb, F. Rehm, H. Reithler, V. Sarkisovi, A. Schmidt, C. Seth, A. Sharma, J.L. Spah, F. Torres Da Silva De Araujo[23], S. Wiedenbeck, S. Zaleski

RWTH Aachen University, III. Physikalisches Institut B, Aachen, Germany
C. Dziwok, G. Flügge, T. Kress, A. Nowack, O. Pooth, A. Stahl, T. Ziemons, A. Zotz

Deutsches Elektronen-Synchrotron, Hamburg, Germany
H. Aarup Petersen, M. Aldaya Martin, J. Alimena, S. Amoroso, Y. An, J. Bach, S. Baxter, M. Bayatmakou, H. Becerril Gonzalez, O. Behnke, A. Belvedere, F. Blekman[24], K. Borras[25], A. Campbell, A. Cardini, F. Colombina, M. De Silva, G. Eckerlin, D. Eckstein, L.I. Estevez Banos, E. Gallo[24], A. Geiser, V. Guglielmi, M. Guthoff, A. Hinzmann, L. Jeppe, B. Kaech, M. Kasemann, C. Kleinwort, R. Kogler, M. Komm, D. Krücker, W. Lange, D. Leyva Pernia, K. Lipka[26], W. Lohmann[27], F. Lorkowski, R. Mankel, I.-A. Melzer-Pellmann, M. Mendizabal Morentin, A.B. Meyer, G. Milella, K. Moral Figueroa, A. Mussgiller, L.P. Nair, J. Niedziela, A. Nürnberg, J. Park, E. Ranken, A. Raspereza, D. Rastorguev, J. Rübenach, L. Rygaard, M. Scham[28,25], S. Schnake[25], P. Schütze, C. Schwanenberger[24], D. Selivanova, K. Sharko, M. Shchedrolosiev, D. Stafford, F. Vazzoler, A. Ventura Barroso, R. Walsh, D. Wang, Q. Wang, K. Wichmann, L. Wiens[25], C. Wissing, Y. Yang, S. Zakharov, A. Zimermmane Castro Santos

University of Hamburg, Hamburg, Germany
A. Albrecht, S. Albrecht, M. Antonello, S. Bollweg, M. Bonanomi, P. Connor, K. El Morabit, Y. Fischer, E. Garutti, A. Grohsjean, J. Haller, D. Hundhausen, H.R. Jabusch, G. Kasieczka, P. Keicher, R. Klanner, W. Korcari, T. Kramer, C.c. Kuo, V. Kutzner, F. Labe, J. Lange, A. Lobanov, C. Matthies, L. Moureaux, M. Mrowietz, A. Nigamova, Y. Nissan, A. Paasch, K.J. Pena Rodriguez, T. Quadfasel, B. Raciti, M. Rieger, D. Savoiu, J. Schindler, P. Schleper, M. Schröder, J. Schwandt, M. Sommerhalder, H. Stadie, G. Steinbrück, A. Tews, B. Wiederspan, M. Wolf

Karlsruher Institut fuer Technologie, Karlsruhe, Germany

S. Brommer, E. Butz, T. Chwalek, A. Dierlamm, G.G. Dincer, U. Elicabuk, N. Faltermann, M. Giffels, A. Gottmann, F. Hartmann[29], R. Hofsaess, M. Horzela, U. Husemann, J. Kieseler, M. Klute, O. Lavoryk, J.M. Lawhorn, M. Link, A. Lintuluoto, S. Maier, S. Mitra, M. Mormile, Th. Müller, M. Neukum, M. Oh, E. Pfeffer, M. Presilla, G. Quast, K. Rabbertz, B. Regnery, R. Schmieder, N. Shadskiy, I. Shvetsov, H.J. Simonis, L. Sowa, L. Stockmeier, K. Tauqeer, M. Toms, B. Topko, N. Trevisani, T. Voigtländer, R.F. Von Cube, J. Von Den Driesch, M. Wassmer, S. Wieland, F. Wittig, R. Wolf, X. Zuo

Institute of Nuclear and Particle Physics (INPP), NCSR Demokritos, Aghia Paraskevi, Greece
G. Anagnostou, G. Daskalakis, A. Kyriakis, A. Papadopoulos[29], A. Stakia

National and Kapodistrian University of Athens, Athens, Greece
G. Melachroinos, Z. Painesis, I. Paraskevas, N. Saoulidou, K. Theofilatos, E. Tziaferi, K. Vellidis, I. Zisopoulos

National Technical University of Athens, Athens, Greece
G. Bakas, T. Chatzistavrou, G. Karapostoli, K. Kousouris, I. Papakrivopoulos, E. Siamarkou, G. Tsipolitis, A. Zacharopoulou

University of Ioánnina, Ioánnina, Greece
I. Bestintzanos, I. Evangelou, C. Foudas, C. Kamtsikis, P. Katsoulis, P. Kokkas, P.G. Kosmoglou Kioseoglou, N. Manthos, I. Papadopoulos, J. Strologas

HUN-REN Wigner Research Centre for Physics, Budapest, Hungary
C. Hajdu, D. Horvath[30,31], K. Márton, A.J. Rádl[32], F. Sikler, V. Veszpremi

MTA-ELTE Lendület CMS Particle and Nuclear Physics Group, Eötvös Loránd University, Budapest, Hungary
M. Csanád, K. Farkas, A. Fehérkuti[33], M.M.A. Gadallah[34], Á. Kadlecsik, P. Major, G. Pásztor, G.I. Veres

Faculty of Informatics, University of Debrecen, Debrecen, Hungary
B. Ujvari, G. Zilizi

HUN-REN ATOMKI - Institute of Nuclear Research, Debrecen, Hungary
G. Bencze, S. Czellar, J. Molnar, Z. Szillasi

Karoly Robert Campus, MATE Institute of Technology, Gyongyos, Hungary
T. Csorgo[33], F. Nemes[33], T. Novak

Panjab University, Chandigarh, India
S. Bansal, S.B. Beri, V. Bhatnagar, G. Chaudhary, S. Chauhan, N. Dhingra[35], A. Kaur, A. Kaur, H. Kaur, M. Kaur, S. Kumar, T. Sheokand, J.B. Singh, A. Singla

University of Delhi, Delhi, India
A. Bhardwaj, A. Chhetri, B.C. Choudhary, A. Kumar, A. Kumar, M. Naimuddin, K. Ranjan, M.K. Saini, S. Saumya

Saha Institute of Nuclear Physics, HBNI, Kolkata, India
S. Baradia, S. Barman[36], S. Bhattacharya, S. Das Gupta, S. Dutta, S. Dutta, S. Sarkar

Indian Institute of Technology Madras, Madras, India
M.M. Ameen, P.K. Behera, S.C. Behera, S. Chatterjee, G. Dash, P. Jana,

P. Kalbhor, S. Kamble, J.R. Komaragiri[37], D. Kumar[37], T. Mishra, B. Parida[38], P.R. Pujahari, N.R. Saha, A. Sharma, A.K. Sikdar, R.K. Singh, P. Verma, S. Verma, A. Vijay

Tata Institute of Fundamental Research-A, Mumbai, India
S. Dugad, G.B. Mohanty, M. Shelake, P. Suryadevara

Tata Institute of Fundamental Research-B, Mumbai, India
A. Bala, S. Banerjee, S. Bhowmik, R.M. Chatterjee, M. Guchait, Sh. Jain, A. Jaiswal, B.M. Joshi, S. Kumar, G. Majumder, K. Mazumdar, S. Parolia, A. Thachayath

National Institute of Science Education and Research, An OCC of Homi Bhabha National Institute, Bhubaneswar, Odisha, India
S. Bahinipati[39], C. Kar, D. Maity[40], P. Mal, K. Naskar[40], A. Nayak[40], S. Nayak, K. Pal, P. Sadangi, S.K. Swain, S. Varghese[40], D. Vats[40]

Indian Institute of Science Education and Research (IISER), Pune, India
S. Acharya[41], A. Alpana, S. Dube, B. Gomber[41], P. Hazarika, B. Kansal, A. Laha, B. Sahu[41], S. Sharma, K.Y. Vaish

Isfahan University of Technology, Isfahan, Iran
H. Bakhshiansohi[42], A. Jafari[43], M. Zeinali[44]

Institute for Research in Fundamental Sciences (IPM), Tehran, Iran
S. Bashiri, S. Chenarani[45], S.M. Etesami, Y. Hosseini, M. Khakzad, E. Khazaie, M. Mohammadi Najafabadi, S. Tizchang[46]

University College Dublin, Dublin, Ireland
M. Felcini, M. Grunewald

INFN Sezione di Bari[a], Università di Bari[b], Politecnico di Bari[c], Bari, Italy
M. Abbrescia[a,b], A. Colaleo[a,b], D. Creanza[a,c], B. D'Anzi[a,b], N. De Filippis[a,c], M. De Palma[a,b], W. Elmetenawee[a,b,47], N. Ferrara[a,b], L. Fiore[a], G. Iaselli[a,c], L. Longo[a], M. Louka[a,b], G. Maggi[a,c], M. Maggi[a], I. Margjeka[a], V. Mastrapasqua[a,b], S. My[a,b], S. Nuzzo[a,b], A. Pellecchia[a,b], A. Pompili[a,b], G. Pugliese[a,c], R. Radogna[a,b], D. Ramos[a], A. Ranieri[a], L. Silvestris[a], F.M. Simone[a,c], Ü. Sözbilir[a], A. Stamerra[a,b], D. Troiano[a,b], R. Venditti[a,b], P. Verwilligen[a], A. Zaza[a,b]

INFN Sezione di Bologna[a], Università di Bologna[b], Bologna, Italy
G. Abbiendi[a], C. Battilana[a,b], D. Bonacorsi[a,b], P. Capiluppi[a,b], A. Castro[†a,b], F.R. Cavallo[a], M. Cuffiani[a,b], G.M. Dallavalle[a], T. Diotalevi[a,b], F. Fabbri[a], A. Fanfani[a,b], D. Fasanella[a], P. Giacomelli[a], L. Giommi[a,b], C. Grandi[a], L. Guiducci[a,b], S. Lo Meo[a,48], M. Lorusso[a,b], L. Lunerti[a], S. Marcellini[a], G. Masetti[a], F.L. Navarria[a,b], G. Paggi[a,b], A. Perrotta[a], F. Primavera[a,b], A.M. Rossi[a,b], S. Rossi Tisbeni[a,b], T. Rovelli[a,b], G.P. Siroli[a,b]

INFN Sezione di Catania[a], Università di Catania[b], Catania, Italy
S. Costa[a,b,49], A. Di Mattia[a], A. Lapertosa[a], R. Potenza[a,b], A. Tricomi[a,b,49]

INFN Sezione di Firenze[a], Università di Firenze[b], Firenze, Italy
P. Assiouras[a], G. Barbagli[a], G. Bardelli[a,b], B. Camaiani[a,b], A. Cassese[a], R. Ceccarelli[a], V. Ciulli[a,b], C. Civinini[a], R. D'Alessandro[a,b], E. Focardi[a,b], T. Kello[a], G. Latino[a,b], P. Lenzi[a,b], M. Lizzo[a], M. Meschini[a], S. Paoletti[a], A. Papanastassiou[a,b], G. Sguazzoni[a], L. Viliani[a]

INFN Laboratori Nazionali di Frascati, Frascati, Italy
L. Benussi, S. Bianco, S. Meola[50], D. Piccolo

INFN Sezione di Genova[a], Università di Genova[b], Genova, Italy
M. Alves Gallo Pereira[a], F. Ferro[a], E. Robutti[a], S. Tosi[a,b]

INFN Sezione di Milano-Bicocca[a], Università di Milano-Bicocca[b], Milano, Italy
A. Benaglia[a], F. Brivio[a], F. Cetorelli[a,b], F. De Guio[a,b], M.E. Dinardo[a,b], P. Dini[a], S. Gennai[a], R. Gerosa[a,b], A. Ghezzi[a,b], P. Govoni[a,b], L. Guzzi[a], G. Lavizzari[a,b], M.T. Lucchini[a,b], M. Malberti[a], S. Malvezzi[a], A. Massironi[a], D. Menasce[a], L. Moroni[a], M. Paganoni[a,b], S. Palluotto[a,b], D. Pedrini[a], A. Perego[a,b], B.S. Pinolini[a], G. Pizzati[a,b], S. Ragazzi[a,b], T. Tabarelli de Fatis[a,b]

INFN Sezione di Napoli[a], Università di Napoli 'Federico II'[b], Napoli, Italy; Università della Basilicata[c], Potenza, Italy; Scuola Superiore Meridionale (SSM)[d], Napoli, Italy
S. Buontempo[a], A. Cagnotta[a,b], F. Carnevali[a,b], N. Cavallo[a,c], F. Fabozzi[a,c], A.O.M. Iorio[a,b], L. Lista[a,b,51], P. Paolucci[a,29], B. Rossi[a]

INFN Sezione di Padova[a], Università di Padova[b], Padova, Italy; Università di Trento[c], Trento, Italy
R. Ardino[a], P. Azzi[a], N. Bacchetta[a,52], D. Bisello[a,b], P. Bortignon[a], G. Bortolato[a,b], A.C.M. Bulla[a], R. Carlin[a,b], P. Checchia[a], T. Dorigo[a], F. Gasparini[a,b], U. Gasparini[a,b], S. Giorgetti[a], E. Lusiani[a], M. Margoni[a,b], M. Michelotto[a], M. Migliorini[a,b], J. Pazzini[a,b], P. Ronchese[a,b], R. Rossin[a,b], F. Simonetto[a,b], M. Tosi[a,b], A. Triossi[a,b], S. Ventura[a], M. Zanetti[a,b], P. Zotto[a,b], A. Zucchetta[a,b], G. Zumerle[a,b]

INFN Sezione di Pavia[a], Università di Pavia[b], Pavia, Italy
A. Braghieri[a], S. Calzaferri[a], D. Fiorina[a], P. Montagna[a,b], V. Re[a], C. Riccardi[a,b], P. Salvini[a], I. Vai[a,b], P. Vitulo[a,b]

INFN Sezione di Perugia[a], Università di Perugia[b], Perugia, Italy
S. Ajmal[a,b], M.E. Ascioti[a,b], G.M. Bilei[a], C. Carrivale[a,b], D. Ciangottini[a,b], L. Fanò[a,b], V. Mariani[a,b], M. Menichelli[a], F. Moscatelli[a,53], A. Rossi[a,b], A. Santocchia[a,b], D. Spiga[a], T. Tedeschi[a,b]

INFN Sezione di Pisa[a], Università di Pisa[b], Scuola Normale Superiore di Pisa[c], Pisa, Italy; Università di Siena[d], Siena, Italy
C. Aimè[a], C.A. Alexe[a,c], P. Asenov[a,b], P. Azzurri[a], G. Bagliesi[a], R. Bhattacharya[a], L. Bianchini[a,b], T. Boccali[a], E. Bossini[a], D. Bruschini[a,c], R. Castaldi[a], M.A. Ciocci[a,b], M. Cipriani[a,b], V. D'Amante[a,d], R. Dell'Orso[a], S. Donato[a], A. Giassi[a], F. Ligabue[a,c], A.C. Marini[a], D. Matos Figueiredo[a], A. Messineo[a,b], S. Mishra[a], V.K. Muraleedharan Nair Bindhu[a,b,40], M. Musich[a,b], S. Nandan[a], F. Palla[a], A. Rizzi[a,b], G. Rolandi[a,c], S. Roy Chowdhury[a], T. Sarkar[a], A. Scribano[a], P. Spagnolo[a], R. Tenchini[a], G. Tonelli[a,b], N. Turini[a,d], F. Vaselli[a,c], A. Venturi[a], P.G. Verdini[a]

INFN Sezione di Roma[a], Sapienza Università di Roma[b], Roma, Italy
P. Barria[a], C. Basile[a,b], F. Cavallari[a], L. Cunqueiro Mendez[a,b], D. Del Re[a,b], E. Di Marco[a,b], M. Diemoz[a], F. Errico[a,b], R. Gargiulo[a,b], E. Longo[a,b], L. Martikainen[a,b], J. Mijuskovic[a,b], G. Organtini[a,b], F. Pandolfi[a], R. Paramatti[a,b], C. Quaranta[a,b], S. Rahatlou[a,b], C. Rovelli[a], F. Santanastasio[a,b], L. Soffi[a], V. Vladimirov[a,b]

INFN Sezione di Torino[a], Università di Torino[b], Torino, Italy; Università del Piemonte Orientale[c], Novara, Italy
N. Amapane[a,b], R. Arcidiacono[a,c], S. Argiro[a,b], M. Arneodo[a,c], N. Bartosik[a], R. Bellan[a,b], C. Biino[a], C. Borca[a,b], N. Cartiglia[a], M. Costa[a,b], R. Covarelli[a,b], N. Demaria[a], L. Finco[a], M. Grippo[a,b], B. Kiani[a,b], F. Legger[a], F. Luongo[a,b], C. Mariotti[a], L. Markovic[a,b], S. Maselli[a], A. Mecca[a,b], L. Menzio[a,b], P. Meridiani[a], E. Migliore[a,b], M. Monteno[a], R. Mulargia[a], M.M. Obertino[a,b], G. Ortona[a], L. Pacher[a,b], N. Pastrone[a], M. Pelliccioni[a], M. Ruspa[a,c], F. Siviero[a,b], V. Sola[a,b], A. Solano[a,b], A. Staiano[a], C. Tarricone[a,b], D. Trocino[a], G. Umoret[a,b], R. White[a,b]

INFN Sezione di Trieste[a], Università di Trieste[b], Trieste, Italy
J. Babbar[a,b], S. Belforte[a], V. Candelise[a,b], M. Casarsa[a], F. Cossutti[a], K. De Leo[a], G. Della Ricca[a,b]

Kyungpook National University, Daegu, Korea
S. Dogra, J. Hong, J. Kim, D. Lee, H. Lee, S.W. Lee, C.S. Moon, Y.D. Oh, M.S. Ryu, S. Sekmen, B. Tae, Y.C. Yang

Department of Mathematics and Physics - GWNU, Gangneung, Korea
M.S. Kim

Chonnam National University, Institute for Universe and Elementary Particles, Kwangju, Korea
G. Bak, P. Gwak, H. Kim, D.H. Moon

Hanyang University, Seoul, Korea
E. Asilar, J. Choi, D. Kim, T.J. Kim, J.A. Merlin, Y. Ryou

Korea University, Seoul, Korea
S. Choi, S. Han, B. Hong, K. Lee, K.S. Lee, S. Lee, J. Yoo

Kyung Hee University, Department of Physics, Seoul, Korea
J. Goh, S. Yang

Sejong University, Seoul, Korea
Y. Kang, H. S. Kim, Y. Kim, S. Lee

Seoul National University, Seoul, Korea
J. Almond, J.H. Bhyun, J. Choi, J. Choi, W. Jun, J. Kim, Y.W. Kim, S. Ko, H. Lee, J. Lee, J. Lee, B.H. Oh, S.B. Oh, H. Seo, U.K. Yang, I. Yoon

University of Seoul, Seoul, Korea
W. Jang, D.Y. Kang, S. Kim, B. Ko, J.S.H. Lee, Y. Lee, I.C. Park, Y. Roh, I.J. Watson

Yonsei University, Department of Physics, Seoul, Korea
S. Ha, K. Hwang, B. Kim, H.D. Yoo

Sungkyunkwan University, Suwon, Korea
M. Choi, M.R. Kim, H. Lee, Y. Lee, I. Yu

College of Engineering and Technology, American University of the Middle East (AUM), Dasman, Kuwait
T. Beyrouthy, Y. Gharbia

Kuwait University - College of Science - Department of Physics, Safat, Kuwait
F. Alazemi

Riga Technical University, Riga, Latvia
K. Dreimanis, A. Gaile, C. Munoz Diaz, D. Osite, G. Pikurs, A. Potrebko, M. Seidel, D. Sidiropoulos Kontos

University of Latvia (LU), Riga, Latvia
N.R. Strautnieks

Vilnius University, Vilnius, Lithuania
M. Ambrozas, A. Juodagalvis, A. Rinkevicius, G. Tamulaitis

National Centre for Particle Physics, Universiti Malaya, Kuala Lumpur, Malaysia
I. Yusuff[54], Z. Zolkapli

Universidad de Sonora (UNISON), Hermosillo, Mexico
J.F. Benitez, A. Castaneda Hernandez, H.A. Encinas Acosta, L.G. Gallegos Maríñez, M. León Coello, J.A. Murillo Quijada, A. Sehrawat, L. Valencia Palomo

Centro de Investigacion y de Estudios Avanzados del IPN, Mexico City, Mexico
G. Ayala, H. Castilla-Valdez, H. Crotte Ledesma, E. De La Cruz-Burelo, I. Heredia-De La Cruz[55], R. Lopez-Fernandez, J. Mejia Guisao, C.A. Mondragon Herrera, A. Sánchez Hernández

Universidad Iberoamericana, Mexico City, Mexico
C. Oropeza Barrera, D.L. Ramirez Guadarrama, M. Ramírez García

Benemerita Universidad Autonoma de Puebla, Puebla, Mexico
I. Bautista, F.E. Neri Huerta, I. Pedraza, H.A. Salazar Ibarguen, C. Uribe Estrada

University of Montenegro, Podgorica, Montenegro
I. Bubanja, N. Raicevic

University of Canterbury, Christchurch, New Zealand
P.H. Butler

National Centre for Physics, Quaid-I-Azam University, Islamabad, Pakistan
A. Ahmad, M.I. Asghar, A. Awais, M.I.M. Awan, H.R. Hoorani, W.A. Khan

AGH University of Krakow, Krakow, Poland
V. Avati, A. Bellora, L. Forthomme, L. Grzanka, M. Malawski, K. Piotrzkowski

National Centre for Nuclear Research, Swierk, Poland
H. Bialkowska, M. Bluj, M. Górski, M. Kazana, M. Szleper, P. Zalewski

Institute of Experimental Physics, Faculty of Physics, University of Warsaw, Warsaw, Poland
K. Bunkowski, K. Doroba, A. Kalinowski, M. Konecki, J. Krolikowski, A. Muhammad

Warsaw University of Technology, Warsaw, Poland
P. Fokow, K. Pozniak, W. Zabolotny

Laboratório de Instrumentação e Física Experimental de Partículas, Lisboa, Portugal
M. Araujo, D. Bastos, C. Beirão Da Cruz E Silva, A. Boletti, M. Bozzo, T. Camporesi, G. Da Molin, P. Faccioli, M. Gallinaro, J. Hollar, N. Leonardo, G.B. Marozzo, A. Petrilli, M. Pisano, J. Seixas, J. Varela, J.W. Wulff

Faculty of Physics, University of Belgrade, Belgrade, Serbia
P. Adzic, P. Milenovic

VINCA Institute of Nuclear Sciences, University of Belgrade, Belgrade, Serbia
D. Devetak, M. Dordevic, J. Milosevic, L. Nadderd, V. Rekovic, M. Stojanovic

Centro de Investigaciones Energéticas Medioambientales y Tecnológicas (CIEMAT), Madrid, Spain
J. Alcaraz Maestre, Cristina F. Bedoya, J.A. Brochero Cifuentes, Oliver M. Carretero, M. Cepeda, M. Cerrada, N. Colino, B. De La Cruz, A. Delgado Peris, A. Escalante Del Valle, D. Fernández Del Val, J.P. Fernández Ramos, J. Flix, M.C. Fouz, O. Gonzalez Lopez, S. Goy Lopez, J.M. Hernandez, M.I. Josa, J. Llorente Merino, C. Martin Perez, E. Martin Viscasillas, D. Moran, C. M. Morcillo Perez, Á. Navarro Tobar, C. Perez Dengra, A. Pérez-Calero Yzquierdo, J. Puerta Pelayo, I. Redondo, J. Sastre, J. Vazquez Escobar

Universidad Autónoma de Madrid, Madrid, Spain
J.F. de Trocóniz

Universidad de Oviedo, Instituto Universitario de Ciencias y Tecnologías Espaciales de Asturias (ICTEA), Oviedo, Spain
B. Alvarez Gonzalez, J. Cuevas, J. Fernandez Menendez, S. Folgueras, I. Gonzalez Caballero, P. Leguina, E. Palencia Cortezon, J. Prado Pico, V. Rodríguez Bouza, A. Soto Rodríguez, A. Trapote, C. Vico Villalba, P. Vischia

Instituto de Física de Cantabria (IFCA), CSIC-Universidad de Cantabria, Santander, Spain
S. Blanco Fernández, I.J. Cabrillo, A. Calderon, J. Duarte Campderros, M. Fernandez, G. Gomez, C. Lasaosa García, R. Lopez Ruiz, C. Martinez Rivero, P. Martinez Ruiz del Arbol, F. Matorras, P. Matorras Cuevas, E. Navarrete Ramos, J. Piedra Gomez, L. Scodellaro, I. Vila, J.M. Vizan Garcia

University of Colombo, Colombo, Sri Lanka
B. Kailasapathy[56], D.D.C. Wickramarathna

University of Ruhuna, Department of Physics, Matara, Sri Lanka
W.G.D. Dharmaratna[57], K. Liyanage, N. Perera

CERN, European Organization for Nuclear Research, Geneva, Switzerland
D. Abbaneo, C. Amendola, E. Auffray, G. Auzinger, J. Baechler, D. Barney, A. Bermúdez Martínez, M. Bianco, A.A. Bin Anuar, A. Bocci, L. Borgonovi, C. Botta, A. Bragagnolo, E. Brondolin, C.E. Brown, C. Caillol, G. Cerminara, N. Chernyavskaya, D. d'Enterria, A. Dabrowski, A. David, A. De Roeck, M.M. Defranchis, M. Deile, M. Dobson, G. Franzoni, W. Funk, S. Giani, D. Gigi, K. Gill, F. Glege, M. Glowacki, J. Hegeman, J.K. Heikkilä, B. Huber, V. Innocente, T. James, P. Janot, O. Kaluzinska, O. Karacheban[27], G. Karathanasis, S. Laurila, P. Lecoq, E. Leutgeb, C. Lourenço, M. Magherini, L. Malgeri, M. Mannelli, M. Matthewman, A. Mehta, F. Meijers, S. Mersi, E. Meschi, V. Milosevic, F. Monti, F. Moortgat, M. Mulders, I. Neutelings, S. Orfanelli, F. Pantaleo, G. Petrucciani, A. Pfeiffer, M. Pierini, M. Pitt, H. Qu, D. Rabady, B. Ribeiro Lopes, F. Riti, M. Rovere, H. Sakulin, R. Salvatico, S. Sanchez Cruz, S. Scarfi, C. Schwick, M. Selvaggi, A. Sharma, K. Shchelina, P. Silva, P. Sphicas[58], A.G. Stahl Leiton, A. Steen, S. Summers, D. Treille, P. Tropea, D. Walter, J. Wanczyk[59], J. Wang, S. Wuchterl, P. Zehetner, P. Zejdl, W.D. Zeuner

PSI Center for Neutron and Muon Sciences, Villigen, Switzerland
T. Bevilacqua[60], L. Caminada[60], A. Ebrahimi, W. Erdmann, R. Horisberger,

Q. Ingram, H.C. Kaestli, D. Kotlinski, C. Lange, M. Missiroli[60], L. Noehte[60], T. Rohe, A. Samalan

ETH Zurich - Institute for Particle Physics and Astrophysics (IPA), Zurich, Switzerland
T.K. Aarrestad, M. Backhaus, G. Bonomelli, A. Calandri, C. Cazzaniga, K. Datta, P. De Bryas Dexmiers D'archiac[59], A. De Cosa, G. Dissertori, M. Dittmar, M. Donegà, F. Eble, M. Galli, K. Gedia, F. Glessgen, C. Grab, N. Härringer, T.G. Harte, D. Hits, W. Lustermann, A.-M. Lyon, R.A. Manzoni, M. Marchegiani, L. Marchese, A. Mascellani[59], F. Nessi-Tedaldi, F. Pauss, V. Perovic, S. Pigazzini, B. Ristic, R. Seidita, J. Steggemann[59], A. Tarabini, D. Valsecchi, R. Wallny

Universität Zürich, Zurich, Switzerland
C. Amsler[61], P. Bärtschi, M.F. Canelli, K. Cormier, M. Huwiler, W. Jin, A. Jofrehei, B. Kilminster, S. Leontsinis, S.P. Liechti, A. Macchiolo, P. Meiring, F. Meng, J. Motta, A. Reimers, P. Robmann, M. Senger, E. Shokr, F. Stäger, R. Tramontano

National Central University, Chung-Li, Taiwan
C. Adloff[62], D. Bhowmik, C.M. Kuo, W. Lin, P.K. Rout, P.C. Tiwari[37]

National Taiwan University (NTU), Taipei, Taiwan
L. Ceard, K.F. Chen, Z.g. Chen, A. De Iorio, W.-S. Hou, T.h. Hsu, Y.w. Kao, S. Karmakar, G. Kole, Y.y. Li, R.-S. Lu, E. Paganis, X.f. Su, J. Thomas-Wilsker, L.s. Tsai, D. Tsionou, H.y. Wu, E. Yazgan

High Energy Physics Research Unit, Department of Physics, Faculty of Science, Chulalongkorn University, Bangkok, Thailand
C. Asawatangtrakuldee, N. Srimanobhas, V. Wachirapusitanand

Tunis El Manar University, Tunis, Tunisia
Y. Maghrbi

Çukurova University, Physics Department, Science and Art Faculty, Adana, Turkey
D. Agyel, F. Boran, F. Dolek, I. Dumanoglu[63], E. Eskut, Y. Guler[64], E. Gurpinar Guler[64], C. Isik, O. Kara, A. Kayis Topaksu, Y. Komurcu, G. Onengut, K. Ozdemir[65], A. Polatoz, B. Tali[66], U.G. Tok, E. Uslan, I.S. Zorbakir

Middle East Technical University, Physics Department, Ankara, Turkey
M. Yalvac[67]

Bogazici University, Istanbul, Turkey
B. Akgun, I.O. Atakisi, E. Gülmez, M. Kaya[68], O. Kaya[69], S. Tekten[70]

Istanbul Technical University, Istanbul, Turkey
A. Cakir, K. Cankocak[63,71], S. Sen[72]

Istanbul University, Istanbul, Turkey
O. Aydilek[73], B. Hacisahinoglu, I. Hos[74], B. Kaynak, S. Ozkorucuklu, O. Potok, H. Sert, C. Simsek, C. Zorbilmez

Yildiz Technical University, Istanbul, Turkey
S. Cerci, B. Isildak[75], D. Sunar Cerci, T. Yetkin

Institute for Scintillation Materials of National Academy of Science of Ukraine, Kharkiv, Ukraine
A. Boyaryntsev, B. Grynyov

National Science Centre, Kharkiv Institute of Physics and Technology, Kharkiv, Ukraine
L. Levchuk

University of Bristol, Bristol, United Kingdom
D. Anthony, J.J. Brooke, A. Bundock, F. Bury, E. Clement, D. Cussans, H. Flacher, J. Goldstein, H.F. Heath, M.-L. Holmberg, L. Kreczko, S. Paramesvaran, L. Robertshaw, V.J. Smith, K. Walkingshaw Pass

Rutherford Appleton Laboratory, Didcot, United Kingdom
A.H. Ball, K.W. Bell, A. Belyaev[76], C. Brew, R.M. Brown, D.J.A. Cockerill, C. Cooke, A. Elliot, K.V. Ellis, K. Harder, S. Harper, J. Linacre, K. Manolopoulos, D.M. Newbold, E. Olaiya, D. Petyt, T. Reis, A.R. Sahasransu, G. Salvi, T. Schuh, C.H. Shepherd-Themistocleous, I.R. Tomalin, K.C. Whalen, T. Williams

Imperial College, London, United Kingdom
I. Andreou, R. Bainbridge, P. Bloch, O. Buchmuller, C.A. Carrillo Montoya, G.S. Chahal[77], D. Colling, J.S. Dancu, I. Das, P. Dauncey, G. Davies, M. Della Negra, S. Fayer, G. Fedi, G. Hall, A. Howard, G. Iles, C.R. Knight, P. Krueper, J. Langford, K.H. Law, J. León Holgado, L. Lyons, A.-M. Magnan, B. Maier, S. Mallios, M. Mieskolainen, J. Nash[78], M. Pesaresi, P.B. Pradeep, B.C. Radburn-Smith, A. Richards, A. Rose, K. Savva, C. Seez, R. Shukla, A. Tapper, K. Uchida, G.P. Uttley, T. Virdee[29], M. Vojinovic, N. Wardle, D. Winterbottom

Brunel University, Uxbridge, United Kingdom
J.E. Cole, A. Khan, P. Kyberd, I.D. Reid

Baylor University, Waco, Texas, USA
S. Abdullin, A. Brinkerhoff, E. Collins, M.R. Darwish, J. Dittmann, K. Hatakeyama, V. Hegde, J. Hiltbrand, B. McMaster, J. Samudio, S. Sawant, C. Sutantawibul, J. Wilson

Catholic University of America, Washington, DC, USA
R. Bartek, A. Dominguez, A.E. Simsek, S.S. Yu

The University of Alabama, Tuscaloosa, Alabama, USA
B. Bam, A. Buchot Perraguin, R. Chudasama, S.I. Cooper, C. Crovella, S.V. Gleyzer, E. Pearson, C.U. Perez, P. Rumerio[79], E. Usai, R. Yi

Boston University, Boston, Massachusetts, USA
A. Akpinar, C. Cosby, G. De Castro, Z. Demiragli, C. Erice, C. Fangmeier, C. Fernandez Madrazo, E. Fontanesi, D. Gastler, F. Golf, S. Jeon, J. O'cain, I. Reed, J. Rohlf, K. Salyer, D. Sperka, D. Spitzbart, I. Suarez, A. Tsatsos, A.G. Zecchinelli

Brown University, Providence, Rhode Island, USA
G. Barone, G. Benelli, D. Cutts, L. Gouskos, M. Hadley, U. Heintz, K.W. Ho, J.M. Hogan[80], T. Kwon, G. Landsberg, K.T. Lau, J. Luo, S. Mondal, T. Russell, S. Sagir[81], X. Shen, M. Stamenkovic, N. Venkatasubramanian

University of California, Davis, Davis, California, USA
S. Abbott, B. Barton, C. Brainerd, R. Breedon, H. Cai, M. Calderon De La Barca Sanchez, M. Chertok, M. Citron, J. Conway, P.T. Cox, R. Erbacher, F. Jensen, O. Kukral, G. Mocellin, M. Mulhearn, S. Ostrom,

W. Wei, S. Yoo, F. Zhang

University of California, Los Angeles, California, USA
K. Adamidis, M. Bachtis, D. Campos, R. Cousins, A. Datta, G. Flores Avila, J. Hauser, M. Ignatenko, M.A. Iqbal, T. Lam, Y.f. Lo, E. Manca, A. Nunez Del Prado, D. Saltzberg, V. Valuev

University of California, Riverside, Riverside, California, USA
R. Clare, J.W. Gary, G. Hanson

University of California, San Diego, La Jolla, California, USA
A. Aportela, A. Arora, J.G. Branson, S. Cittolin, S. Cooperstein, D. Diaz, J. Duarte, L. Giannini, Y. Gu, J. Guiang, R. Kansal, V. Krutelyov, R. Lee, J. Letts, M. Masciovecchio, F. Mokhtar, S. Mukherjee, M. Pieri, D. Primosch, M. Quinnan, V. Sharma, M. Tadel, E. Vourliotis, F. Würthwein, Y. Xiang, A. Yagil

University of California, Santa Barbara - Department of Physics, Santa Barbara, California, USA
A. Barzdukas, L. Brennan, C. Campagnari, K. Downham, C. Grieco, M.M. Hussain, J. Incandela, J. Kim, A.J. Li, P. Masterson, H. Mei, J. Richman, S.N. Santpur, U. Sarica, R. Schmitz, F. Setti, J. Sheplock, D. Stuart, T.Á. Vámi, X. Yan, D. Zhang

California Institute of Technology, Pasadena, California, USA
S. Bhattacharya, A. Bornheim, O. Cerri, J. Mao, H.B. Newman, G. Reales Gutiérrez, M. Spiropulu, J.R. Vlimant, C. Wang, S. Xie, R.Y. Zhu

Carnegie Mellon University, Pittsburgh, Pennsylvania, USA
J. Alison, S. An, P. Bryant, M. Cremonesi, V. Dutta, T. Ferguson, T.A. Gómez Espinosa, A. Harilal, A. Kallil Tharayil, M. Kanemura, C. Liu, T. Mudholkar, S. Murthy, P. Palit, K. Park, M. Paulini, A. Roberts, A. Sanchez, W. Terrill

University of Colorado Boulder, Boulder, Colorado, USA
J.P. Cumalat, W.T. Ford, A. Hart, A. Hassani, N. Manganelli, J. Pearkes, C. Savard, N. Schonbeck, K. Stenson, K.A. Ulmer, S.R. Wagner, N. Zipper, D. Zuolo

Cornell University, Ithaca, New York, USA
J. Alexander, X. Chen, D.J. Cranshaw, J. Dickinson, J. Fan, X. Fan, S. Hogan, P. Kotamnives, J. Monroy, M. Oshiro, J.R. Patterson, M. Reid, A. Ryd, J. Thom, P. Wittich, R. Zou

Fermi National Accelerator Laboratory, Batavia, Illinois, USA
M. Albrow, M. Alyari, O. Amram, G. Apollinari, A. Apresyan, L.A.T. Bauerdick, D. Berry, J. Berryhill, P.C. Bhat, K. Burkett, J.N. Butler, A. Canepa, G.B. Cerati, H.W.K. Cheung, F. Chlebana, G. Cummings, I. Dutta, V.D. Elvira, J. Freeman, A. Gandrakota, Z. Gecse, L. Gray, D. Green, A. Grummer, S. Grünendahl, D. Guerrero, O. Gutsche, R.M. Harris, T.C. Herwig, J. Hirschauer, B. Jayatilaka, S. Jindariani, M. Johnson, U. Joshi, T. Klijnsma, B. Klima, K.H.M. Kwok, S. Lammel, C. Lee, D. Lincoln, R. Lipton, T. Liu, K. Maeshima, D. Mason, P. McBride, P. Merkel, S. Mrenna, S. Nahn, J. Ngadiuba, D. Noonan, S. Norberg, V. Papadimitriou, N. Pastika, K. Pedro, C. Pena[82], F. Ravera, A. Reinsvold Hall[83], L. Ristori, M. Safdari, E. Sexton-Kennedy, N. Smith,

A. Soha, L. Spiegel, S. Stoynev, J. Strait, L. Taylor, S. Tkaczyk, N.V. Tran, L. Uplegger, E.W. Vaandering, I. Zoi

University of Florida, Gainesville, Florida, USA
C. Aruta, P. Avery, D. Bourilkov, P. Chang, V. Cherepanov, R.D. Field, C. Huh, E. Koenig, M. Kolosova, J. Konigsberg, A. Korytov, K. Matchev, N. Menendez, G. Mitselmakher, K. Mohrman, A. Muthirakalayil Madhu, N. Rawal, S. Rosenzweig, Y. Takahashi, J. Wang

Florida State University, Tallahassee, Florida, USA
T. Adams, A. Al Kadhim, A. Askew, S. Bower, R. Hashmi, R.S. Kim, S. Kim, T. Kolberg, G. Martinez, H. Prosper, P.R. Prova, M. Wulansatiti, R. Yohay, J. Zhang

Florida Institute of Technology, Melbourne, Florida, USA
B. Alsufyani, S. Butalla, S. Das, T. Elkafrawy[18], M. Hohlmann, E. Yanes

University of Illinois Chicago, Chicago, Illinois, USA
M.R. Adams, A. Baty, C. Bennett, R. Cavanaugh, R. Escobar Franco, O. Evdokimov, C.E. Gerber, M. Hawksworth, A. Hingrajiya, D.J. Hofman, J.h. Lee, D. S. Lemos, C. Mills, S. Nanda, G. Oh, B. Ozek, D. Pilipovic, R. Pradhan, E. Prifti, T. Roy, S. Rudrabhatla, N. Singh, M.B. Tonjes, N. Varelas, M.A. Wadud, Z. Ye, J. Yoo

The University of Iowa, Iowa City, Iowa, USA
M. Alhusseini, D. Blend, K. Dilsiz[84], L. Emediato, G. Karaman, O.K. Köseyan, J.-P. Merlo, A. Mestvirishvili[85], O. Neogi, H. Ogul[86], Y. Onel, A. Penzo, C. Snyder, E. Tiras[87]

Johns Hopkins University, Baltimore, Maryland, USA
B. Blumenfeld, L. Corcodilos, J. Davis, A.V. Gritsan, L. Kang, S. Kyriacou, P. Maksimovic, M. Roguljic, J. Roskes, S. Sekhar, M. Swartz

The University of Kansas, Lawrence, Kansas, USA
A. Abreu, L.F. Alcerro Alcerro, J. Anguiano, S. Arteaga Escatel, P. Baringer, A. Bean, Z. Flowers, D. Grove, J. King, G. Krintiras, M. Lazarovits, C. Le Mahieu, J. Marquez, M. Murray, M. Nickel, S. Popescu[88], C. Rogan, C. Royon, S. Sanders, C. Smith, G. Wilson

Kansas State University, Manhattan, Kansas, USA
B. Allmond, R. Gujju Gurunadha, A. Ivanov, K. Kaadze, Y. Maravin, J. Natoli, D. Roy, G. Sorrentino

University of Maryland, College Park, Maryland, USA
A. Baden, A. Belloni, J. Bistany-riebman, Y.M. Chen, S.C. Eno, N.J. Hadley, S. Jabeen, R.G. Kellogg, T. Koeth, B. Kronheim, Y. Lai, S. Lascio, A.C. Mignerey, S. Nabili, C. Palmer, C. Papageorgakis, M.M. Paranjpe, E. Popova[89], A. Shevelev, L. Wang, L. Zhang

Massachusetts Institute of Technology, Cambridge, Massachusetts, USA
C. Baldenegro Barrera, J. Bendavid, S. Bright-Thonney, I.A. Cali, P.c. Chou, M. D'Alfonso, J. Eysermans, C. Freer, G. Gomez-Ceballos, M. Goncharov, G. Grosso, P. Harris, D. Hoang, D. Kovalskyi, J. Krupa, L. Lavezzo, Y.-J. Lee, K. Long, C. Mcginn, A. Novak, M.I. Park, C. Paus, C. Reissel, C. Roland, G. Roland, S. Rothman, G.S.F. Stephans, Z. Wang, B. Wyslouch, T. J. Yang

University of Minnesota, Minneapolis, Minnesota, USA
B. Crossman, C. Kapsiak, M. Krohn, D. Mahon, J. Mans, B. Marzocchi, M. Revering, R. Rusack, R. Saradhy, N. Strobbe

University of Nebraska-Lincoln, Lincoln, Nebraska, USA
K. Bloom, D.R. Claes, G. Haza, J. Hossain, C. Joo, I. Kravchenko, A. Rohilla, J.E. Siado, W. Tabb, A. Vagnerini, A. Wightman, F. Yan, D. Yu

State University of New York at Buffalo, Buffalo, New York, USA
H. Bandyopadhyay, L. Hay, H.w. Hsia, I. Iashvili, A. Kalogeropoulos, A. Kharchilava, M. Morris, D. Nguyen, S. Rappoccio, H. Rejeb Sfar, A. Williams, P. Young

Northeastern University, Boston, Massachusetts, USA
G. Alverson, E. Barberis, J. Bonilla, B. Bylsma, M. Campana, J. Dervan, Y. Haddad, Y. Han, I. Israr, A. Krishna, P. Levchenko, J. Li, M. Lu, R. Mccarthy, D.M. Morse, V. Nguyen, T. Orimoto, A. Parker, L. Skinnari, E. Tsai, D. Wood

Northwestern University, Evanston, Illinois, USA
S. Dittmer, K.A. Hahn, D. Li, Y. Liu, M. Mcginnis, Y. Miao, D.G. Monk, M.H. Schmitt, A. Taliercio, M. Velasco

University of Notre Dame, Notre Dame, Indiana, USA
G. Agarwal, R. Band, R. Bucci, S. Castells, A. Das, R. Goldouzian, M. Hildreth, K. Hurtado Anampa, T. Ivanov, C. Jessop, K. Lannon, J. Lawrence, N. Loukas, L. Lutton, J. Mariano, N. Marinelli, I. Mcalister, T. McCauley, C. Mcgrady, C. Moore, Y. Musienko[15], H. Nelson, M. Osherson, A. Piccinelli, R. Ruchti, A. Townsend, Y. Wan, M. Wayne, H. Yockey, M. Zarucki, L. Zygala

The Ohio State University, Columbus, Ohio, USA
A. Basnet, M. Carrigan, L.S. Durkin, C. Hill, M. Joyce, M. Nunez Ornelas, K. Wei, D.A. Wenzl, B.L. Winer, B. R. Yates

Princeton University, Princeton, New Jersey, USA
H. Bouchamaoui, K. Coldham, P. Das, G. Dezoort, P. Elmer, P. Fackeldey, A. Frankenthal, B. Greenberg, N. Haubrich, K. Kennedy, G. Kopp, S. Kwan, D. Lange, A. Loeliger, D. Marlow, I. Ojalvo, J. Olsen, F. Simpson, D. Stickland, C. Tully, L.H. Vage

University of Puerto Rico, Mayaguez, Puerto Rico, USA
S. Malik, R. Sharma

Purdue University, West Lafayette, Indiana, USA
A.S. Bakshi, S. Chandra, R. Chawla, A. Gu, L. Gutay, M. Jones, A.W. Jung, A.M. Koshy, M. Liu, G. Negro, N. Neumeister, G. Paspalaki, S. Piperov, J.F. Schulte, A. K. Virdi, F. Wang, A. Wildridge, W. Xie, Y. Yao

Purdue University Northwest, Hammond, Indiana, USA
J. Dolen, N. Parashar, A. Pathak

Rice University, Houston, Texas, USA
D. Acosta, A. Agrawal, T. Carnahan, K.M. Ecklund, P.J. Fernández Manteca, S. Freed, P. Gardner, F.J.M. Geurts, I. Krommydas, W. Li, J. Lin, O. Miguel Colin, B.P. Padley, R. Redjimi, J. Rotter, E. Yigitbasi, Y. Zhang

University of Rochester, Rochester, New York, USA
A. Bodek, P. de Barbaro, R. Demina, J.L. Dulemba, A. Garcia-Bellido, O. Hindrichs, A. Khukhunaishvili, N. Parmar, P. Parygin[89], R. Taus

Rutgers, The State University of New Jersey, Piscataway, New Jersey, USA
B. Chiarito, J.P. Chou, S.V. Clark, D. Gadkari, Y. Gershtein, E. Halkiadakis, M. Heindl, C. Houghton, D. Jaroslawski, S. Konstantinou, I. Laflotte, A. Lath, R. Montalvo, K. Nash, J. Reichert, P. Saha, S. Salur, S. Schnetzer, S. Somalwar, R. Stone, S.A. Thayil, S. Thomas, J. Vora

University of Tennessee, Knoxville, Tennessee, USA
D. Ally, A.G. Delannoy, S. Fiorendi, S. Higginbotham, T. Holmes, A.R. Kanuganti, N. Karunarathna, L. Lee, E. Nibigira, S. Spanier

Texas A&M University, College Station, Texas, USA
D. Aebi, M. Ahmad, T. Akhter, K. Androsov[59], O. Bouhali[90], R. Eusebi, J. Gilmore, T. Huang, T. Kamon[91], H. Kim, S. Luo, R. Mueller, D. Overton, A. Safonov

Texas Tech University, Lubbock, Texas, USA
N. Akchurin, J. Damgov, Y. Feng, N. Gogate, Y. Kazhykarim, K. Lamichhane, S.W. Lee, C. Madrid, A. Mankel, T. Peltola, I. Volobouev

Vanderbilt University, Nashville, Tennessee, USA
E. Appelt, Y. Chen, S. Greene, A. Gurrola, W. Johns, R. Kunnawalkam Elayavalli, A. Melo, D. Rathjens, F. Romeo, P. Sheldon, S. Tuo, J. Velkovska, J. Viinikainen

University of Virginia, Charlottesville, Virginia, USA
B. Cardwell, H. Chung, B. Cox, J. Hakala, R. Hirosky, A. Ledovskoy, C. Mantilla, C. Neu, C. Ramón Álvarez

Wayne State University, Detroit, Michigan, USA
S. Bhattacharya, P.E. Karchin

University of Wisconsin - Madison, Madison, Wisconsin, USA
A. Aravind, S. Banerjee, K. Black, T. Bose, E. Chavez, S. Dasu, P. Everaerts, C. Galloni, H. He, M. Herndon, A. Herve, C.K. Koraka, A. Lanaro, R. Loveless, J. Madhusudanan Sreekala, A. Mallampalli, A. Mohammadi, S. Mondal, G. Parida, L. Pétré, D. Pinna, A. Savin, V. Shang, V. Sharma, W.H. Smith, D. Teague, H.F. Tsoi, W. Vetens, A. Warden

Authors affiliated with an international laboratory covered by a cooperation agreement with CERN
G. Gavrilov, V. Golovtcov, Y. Ivanov, V. Kim[92], V. Murzin, V. Oreshkin, D. Sosnov, V. Sulimov, L. Uvarov, A. Vorobyev[†], T. Aushev, K. Ivanov

Authors affiliated with an institute formerly covered by a cooperation agreement with CERN
S. Afanasiev, V. Alexakhin, D. Budkouski, I. Golutvin[†], I. Gorbunov, V. Karjavine, O. Kodolova[93,89], V. Korenkov, A. Lanev, A. Malakhov, V. Matveev[92], A. Nikitenko[94,93], V. Palichik, V. Perelygin, M. Savina, V. Shalaev, S. Shmatov, S. Shulha, V. Smirnov, O. Teryaev, N. Voytishin, B.S. Yuldashev[†95], A. Zarubin, I. Zhizhin, Yu. Andreev, A. Dermenev, S. Gninenko, N. Golubev, A. Karneyeu, D. Kirpichnikov, M. Kirsanov, N. Krasnikov, I. Tlisova, A. Toropin, V. Gavrilov, N. Lychkovskaya, V. Popov, A. Zhokin, R. Chistov[92], M. Danilov[96],

S. Polikarpov[92], V. Andreev, M. Azarkin, M. Kirakosyan, A. Terkulov, E. Boos, V. Bunichev, M. Dubinin[82], L. Dudko, V. Klyukhin, M. Perfilov, S. Petrushanko, V. Savrin, A. Snigirev, G. Vorotnikov, V. Blinov[92], T. Dimova[92], A. Kozyrev[92], O. Radchenko[92], Y. Skovpen[92], V. Kachanov, S. Slabospitskii, A. Uzunian, A. Babaev, V. Borshch, D. Druzhkin[97]

†: Deceased
[1]Also at Yerevan State University, Yerevan, Armenia
[2]Also at TU Wien, Vienna, Austria
[3]Also at Ghent University, Ghent, Belgium
[4]Also at Universidade do Estado do Rio de Janeiro, Rio de Janeiro, Brazil
[5]Also at FACAMP - Faculdades de Campinas, Sao Paulo, Brazil
[6]Also at Universidade Estadual de Campinas, Campinas, Brazil
[7]Also at Federal University of Rio Grande do Sul, Porto Alegre, Brazil
[8]Also at University of Chinese Academy of Sciences, Beijing, China
[9]Also at China Center of Advanced Science and Technology, Beijing, China
[10]Also at University of Chinese Academy of Sciences, Beijing, China
[11]Also at China Spallation Neutron Source, Guangdong, China
[12]Now at Henan Normal University, Xinxiang, China
[13]Also at University of Shanghai for Science and Technology, Shanghai, China
[14]Now at The University of Iowa, Iowa City, Iowa, USA
[15]Also at an institute formerly covered by a cooperation agreement with CERN
[16]Also at Zewail City of Science and Technology, Zewail, Egypt
[17]Also at British University in Egypt, Cairo, Egypt
[18]Now at Ain Shams University, Cairo, Egypt
[19]Also at Purdue University, West Lafayette, Indiana, USA
[20]Also at Université de Haute Alsace, Mulhouse, France
[21]Also at Istinye University, Istanbul, Turkey
[22]Also at Tbilisi State University, Tbilisi, Georgia
[23]Also at The University of the State of Amazonas, Manaus, Brazil
[24]Also at University of Hamburg, Hamburg, Germany
[25]Also at RWTH Aachen University, III. Physikalisches Institut A, Aachen, Germany
[26]Also at Bergische University Wuppertal (BUW), Wuppertal, Germany
[27]Also at Brandenburg University of Technology, Cottbus, Germany
[28]Also at Forschungszentrum Jülich, Juelich, Germany
[29]Also at CERN, European Organization for Nuclear Research, Geneva, Switzerland
[30]Also at HUN-REN ATOMKI - Institute of Nuclear Research, Debrecen, Hungary
[31]Now at Universitatea Babes-Bolyai - Facultatea de Fizica, Cluj-Napoca, Romania
[32]Also at MTA-ELTE Lendület CMS Particle and Nuclear Physics Group, Eötvös Loránd University, Budapest, Hungary
[33]Also at HUN-REN Wigner Research Centre for Physics, Budapest, Hungary
[34]Also at Physics Department, Faculty of Science, Assiut University, Assiut, Egypt
[35]Also at Punjab Agricultural University, Ludhiana, India
[36]Also at University of Visva-Bharati, Santiniketan, India
[37]Also at Indian Institute of Science (IISc), Bangalore, India
[38]Also at Amity University Uttar Pradesh, Noida, India
[39]Also at IIT Bhubaneswar, Bhubaneswar, India
[40]Also at Institute of Physics, Bhubaneswar, India
[41]Also at University of Hyderabad, Hyderabad, India
[42]Also at Deutsches Elektronen-Synchrotron, Hamburg, Germany

[43]Also at Isfahan University of Technology, Isfahan, Iran
[44]Also at Sharif University of Technology, Tehran, Iran
[45]Also at Department of Physics, University of Science and Technology of Mazandaran, Behshahr, Iran
[46]Also at Department of Physics, Faculty of Science, Arak University, ARAK, Iran
[47]Also at Helwan University, Cairo, Egypt
[48]Also at Italian National Agency for New Technologies, Energy and Sustainable Economic Development, Bologna, Italy
[49]Also at Centro Siciliano di Fisica Nucleare e di Struttura Della Materia, Catania, Italy
[50]Also at Università degli Studi Guglielmo Marconi, Roma, Italy
[51]Also at Scuola Superiore Meridionale, Università di Napoli 'Federico II', Napoli, Italy
[52]Also at Fermi National Accelerator Laboratory, Batavia, Illinois, USA
[53]Also at Consiglio Nazionale delle Ricerche - Istituto Officina dei Materiali, Perugia, Italy
[54]Also at Department of Applied Physics, Faculty of Science and Technology, Universiti Kebangsaan Malaysia, Bangi, Malaysia
[55]Also at Consejo Nacional de Ciencia y Tecnología, Mexico City, Mexico
[56]Also at Trincomalee Campus, Eastern University, Sri Lanka, Nilaveli, Sri Lanka
[57]Also at Saegis Campus, Nugegoda, Sri Lanka
[58]Also at National and Kapodistrian University of Athens, Athens, Greece
[59]Also at Ecole Polytechnique Fédérale Lausanne, Lausanne, Switzerland
[60]Also at Universität Zürich, Zurich, Switzerland
[61]Also at Stefan Meyer Institute for Subatomic Physics, Vienna, Austria
[62]Also at Laboratoire d'Annecy-le-Vieux de Physique des Particules, IN2P3-CNRS, Annecy-le-Vieux, France
[63]Also at Near East University, Research Center of Experimental Health Science, Mersin, Turkey
[64]Also at Konya Technical University, Konya, Turkey
[65]Also at Izmir Bakircay University, Izmir, Turkey
[66]Also at Adiyaman University, Adiyaman, Turkey
[67]Also at Bozok Universitetesi Rektörlügü, Yozgat, Turkey
[68]Also at Marmara University, Istanbul, Turkey
[69]Also at Milli Savunma University, Istanbul, Turkey
[70]Also at Kafkas University, Kars, Turkey
[71]Now at Istanbul Okan University, Istanbul, Turkey
[72]Also at Hacettepe University, Ankara, Turkey
[73]Also at Erzincan Binali Yildirim University, Erzincan, Turkey
[74]Also at Istanbul University - Cerrahpasa, Faculty of Engineering, Istanbul, Turkey
[75]Also at Yildiz Technical University, Istanbul, Turkey
[76]Also at School of Physics and Astronomy, University of Southampton, Southampton, United Kingdom
[77]Also at IPPP Durham University, Durham, United Kingdom
[78]Also at Monash University, Faculty of Science, Clayton, Australia
[79]Also at Università di Torino, Torino, Italy
[80]Also at Bethel University, St. Paul, Minnesota, USA
[81]Also at Karamanoğlu Mehmetbey University, Karaman, Turkey
[82]Also at California Institute of Technology, Pasadena, California, USA
[83]Also at United States Naval Academy, Annapolis, Maryland, USA
[84]Also at Bingol University, Bingol, Turkey
[85]Also at Georgian Technical University, Tbilisi, Georgia

[86]Also at Sinop University, Sinop, Turkey
[87]Also at Erciyes University, Kayseri, Turkey
[88]Also at Horia Hulubei National Institute of Physics and Nuclear Engineering (IFIN-HH), Bucharest, Romania
[89]Now at another institute formerly covered by a cooperation agreement with CERN
[90]Also at Texas A&M University at Qatar, Doha, Qatar
[91]Also at Kyungpook National University, Daegu, Korea
[92]Also at another institute formerly covered by a cooperation agreement with CERN
[93]Also at Yerevan Physics Institute, Yerevan, Armenia
[94]Also at Imperial College, London, United Kingdom
[95]Also at Institute of Nuclear Physics of the Uzbekistan Academy of Sciences, Tashkent, Uzbekistan
[96]Also at another international laboratory covered by a cooperation agreement with CERN
[97]Also at Universiteit Antwerpen, Antwerpen, Belgium